



Published in final edited form as:

*Nat Rev Cancer*. 2017 November ; 17(11): 659–675. doi:10.1038/nrc.2017.83.

## Engineering and physical sciences in oncology: challenges and opportunities

Michael J. Mitchell<sup>1,2</sup>, Rakesh K. Jain<sup>3</sup>, and Robert Langer<sup>2</sup>

<sup>1</sup>Department of Bioengineering, University of Pennsylvania, 240 Skirkanich Hall, 210 S. 33rd Street, Philadelphia, Pennsylvania 19104, USA.

<sup>2</sup>Department of Chemical Engineering, David H. Koch Institute for Integrated Cancer Research, Massachusetts Institute of Technology, 77 Massachusetts Avenue, Cambridge, Massachusetts 02139, USA.

<sup>3</sup>Edwin L. Steele Laboratories of Tumour Biology, Department of Radiation Oncology, Massachusetts General Hospital and Harvard Medical School, 100 Blossom Street, Cox 7, Boston, Massachusetts 02114, USA.

### Abstract

The principles of engineering and physics have been applied to oncology for nearly 50 years. Engineers and physical scientists have made contributions to all aspects of cancer biology, from quantitative understanding of tumour growth and progression to improved detection and treatment of cancer. Many early efforts focused on experimental and computational modelling of drug distribution, cell cycle kinetics and tumour growth dynamics. In the past decade, we have witnessed exponential growth at the interface of engineering, physics and oncology that has been fuelled by advances in fields including materials science, microfabrication, nanomedicine, microfluidics, imaging, and catalysed by new programmes at the National Institutes of Health (NIH), including the National Institute of Biomedical Imaging and Bioengineering (NIBIB), Physical Sciences in Oncology, and the National Cancer Institute (NCI) Alliance for Nanotechnology. Here, we review the advances made at the interface of engineering and physical sciences and oncology in four important areas: the physical microenvironment of the tumour and technological advances in drug delivery; cellular and molecular imaging; and microfluidics and microfabrication. We discuss the research advances, opportunities and challenges for integrating engineering and physical sciences with oncology to develop new methods to study, detect and treat cancer, and we also describe the future outlook for these emerging areas.

---

In addition to biochemical and genetic abnormalities, tumours generate and exert physical forces during growth, progression, and metastasis<sup>1,2</sup>. These physical forces compress blood and lymphatic vessels, thereby reducing perfusion rates and generating hypoxia. In turn, these conditions promote tumour progression and metastasis, contribute to immune evasion

### Author contributions

M.J.M., R.K.J. and R.L. conceived the ideas, researched the data for the manuscript, discussed the manuscript content and wrote the manuscript. M.J.M. designed the display items. All authors reviewed and edited the article before submission.

### Competing interests statement

The authors declare no competing interests.

and reduce the efficacy of therapeutics<sup>1</sup>. In combination with a stiffened extracellular matrix (ECM), physical forces generated by tumours act to increase invasive and metastatic potential<sup>3</sup>. Both malignant and non-malignant cells in the surrounding stroma proliferate and pull on the structural components of the tumour microenvironment (TME) to alter gene expression and cellular signalling<sup>1,4</sup>. Tumour vessels that nourish tumours are leaky and disorganized in part due to these forces, which further decrease perfusion<sup>5</sup>. Vessel leakiness and lymphatic compression together elevate interstitial fluid pressure (IFP) in tumours<sup>1</sup>. These structural and functional abnormalities hinder delivery of systemically administered targeted therapies and nanotherapeutics and lower the efficacy of chemotherapeutic agents, radiotherapy and immunotherapies<sup>5,6</sup>. Additionally, shear forces exerted by flowing blood and interstitial fluids modulate the behaviour of tumour cells and the surrounding TME<sup>1,7</sup>. By detecting and quantifying these physical abnormalities, physical scientists and engineers in collaboration with cancer biologists and oncologists are identifying new therapeutic strategies for cancer<sup>5,6</sup>.

Progress in cancer treatment relies on the development of new technologies originating from engineering and the physical sciences. The first researcher to coin the term ‘chemotherapy’ was a German chemist, Paul Ehrlich, who in 1908 first demonstrated the efficacy of animal models to screen chemicals for their activity against disease<sup>8</sup>. His accomplishments had major ramifications for the development of cancer chemotherapeutic agents, which now rely on collaborations between oncologists and medicinal chemists. In radiation therapy, oncologists work closely with physicists to ensure that patients receive prescribed radiation doses and dose distributions within acceptable degrees of accuracy that spare essential normal tissues. Radiation therapy has been continuously evolving with the development of new radiation techniques and advanced imaging modalities developed by physicists and oncologists in a collaborative effort<sup>9</sup>. In addition to traditional forms of treatment, novel targeted therapies are being developed by engineers to improve drug formulation and delivery, such as those that adapt to, exploit or ‘normalize’ the TME and have the potential to improve the outcome of radiation, chemotherapy, and immunotherapy<sup>6,10–12</sup>. Specifically, chemotherapy has improved, and molecularly targeted therapeutics that rely heavily on advances in engineering are now being used in the clinic owing to new delivery formulations with reduced toxicity<sup>13,14</sup>. Additionally, high-throughput microfabricated drug screening platforms are being developed to identify biomarkers and to test drug responses during the course of personalized therapy<sup>15</sup>. Engineers and mathematicians are also using these technologies to develop pharmacokinetic models to predict drug distribution and efficacy<sup>16</sup>.

In this Review, we provide recent examples to illustrate how engineering and the physical sciences have contributed to the improved detection, treatment and fundamental understanding of cancer in four key areas. These areas are: the physical microenvironment of the tumour; drug delivery; cellular and molecular imaging; and microfluidics and microfabrication specifically applied to cancer.

## Physical microenvironment of the tumour

Engineers and physical scientists have pioneered research into our understanding that cancer is more than simply malignant cells with genetic mutations but can instead be viewed as aberrant organs composed of cancer cells and their surrounding stroma, referred to as the TME<sup>3,6,17–19</sup>. Many aspects of the TME are abnormal, fuelling tumour progression and treatment resistance<sup>6,20–22</sup>.

### Vascular and interstitial barriers

Despite the development of many cancer therapeutics in recent years, physical barriers in the TME limit drug delivery<sup>13,23</sup>. A meta-analysis of 117 studies of nanomedicine delivery showed that only 0.7% (median) of administered nanoparticle dosages reached tumour sites<sup>24</sup>. Nanomedicine delivery to tumours is thought to rely on the enhanced permeability and retention (EPR) effect<sup>25,26</sup>. Studies since these initial descriptions of the EPR effect have further elucidated EPR mechanisms in animal models, including imbalances between proangiogenic and antiangiogenic signalling<sup>6,27</sup>, impaired recruitment of pericytes<sup>28</sup> and collapsed tumour lymphatics<sup>29</sup>. While similar EPR pathophysiology is observed in humans, its benefits remain unclear, as most nanotherapies have not demonstrated substantial benefits over conventional chemotherapy<sup>30</sup>. Evidence suggests that EPR is active in cancer patients, but physiological barriers exist that counteract it<sup>13,31</sup>. In fact, larger nanoparticles (~100 nm diameter) can extravasate from leaky tumour vessels but cannot penetrate through dense ECM, resulting in perivascular localization<sup>32</sup>. Nanoparticles may remain there, but chemotherapeutic agents released from these perivascular ‘depots’ either return to the circulation or advance minimally into tumour tissue, as they largely bind to the first cells they encounter<sup>23</sup>.

Recent work using advanced *in vivo* imaging, computational modelling and animal models has identified barriers in the TME that hinder therapeutic delivery and promote tumour progression<sup>1,5</sup>. These approaches have shown that leaky, disorganized vessels contribute to increased IFP and reduced blood supply to tumours<sup>6</sup>. Increased IFP abolished convective transport of drugs across vessel walls and tumour tissue, limiting penetration of drugs to diffusion alone<sup>33,6</sup> (FIG. 1). To improve therapeutic delivery and slow tumour progression, strategies to normalize vasculature and lower IFP have been investigated. Antiangiogenic therapies such as blocking antibodies against vascular endothelial growth factor receptors (VEGFRs) prune immature tumour vessels and reduce leakiness of the remaining vasculature to improve integrity and function<sup>34</sup>. Specifically, treatment of tumour vasculature with VEGFR2 blocking antibodies improved smaller (~10 nm diameter) nanoparticle delivery, with no improvement for larger (~100 nm diameter) nanoparticles<sup>14</sup>. Mathematical models showed that reductions in vessel wall pore size through vascular normalization with VEGFR2 antibody treatment reduced IFP and improved small nanoparticle penetration<sup>14</sup>. In several clinical trials, vascular normalization with agents that target VEGF or its receptors in combination with chemotherapy and/or radiation therapy is associated with the survival of patients with various tumour types<sup>5</sup>, including glioblastoma<sup>35</sup>, non-small-cell lung cancer (NSCLC)<sup>36</sup>, and breast cancer<sup>37</sup>; the extended patient survival observed in these clinical trials is potentially due to improved vascular

function as determined through measurement of vascular parameters by immunohistochemistry, magnetic resonance imaging (MRI), and/or computed tomography (CT) (NCT00662506; NCT00642759)<sup>38,39</sup>. In fact, vascular normalization contributes to improved survival with more than a dozen approved cancer drugs that block VEGF signalling, including the VEGFA blocking antibody bevacizumab (Avastin; Genentech)<sup>5</sup>.

Normalized vasculature and improved therapeutic delivery can also be achieved by targeting other components of the TME. Alterations in the ECM together with proliferating tumour and stromal cells leads to accumulation of solid stresses independent of IFP, which compress vessels<sup>29,40,41</sup>. These forces have been quantified using mathematical modelling and tumour deformation assays<sup>41,42</sup>. Depletion of tumour cells, cancer-associated fibroblasts (CAFs), or ECM showed that all three components contribute to solid stress accumulation in tumours in mice<sup>40,41</sup>. Obesity also contributes to vessel compression and poor vascular perfusion in pancreatic ductal adenocarcinoma (PDAC), as pancreatic tumours in obese mice have increased numbers of neutrophils, pancreatic stellate cells and adipocytes, creating a denser microenvironment<sup>43</sup>. Treatment with losartan, a clinically approved angiotensin II receptor antagonist shown to reduce desmoplasia<sup>6</sup>, also reduced solid stresses and pancreatic tumour progression in mice<sup>43</sup>. Moreover, angiotensin system inhibitors including losartan can also activate both innate and adaptive immune pathways in patients with PDAC<sup>44</sup>. The feasibility of using losartan to treat patients with pancreatic cancer was demonstrated in a phase II clinical trial (NCT01821729)<sup>45,46</sup>.

### ECM stiffening

Human tumour tissue is often stiffer than normal tissue due to numerous factors, including desmoplasia and ECM reorganization and crosslinking. Cells including CAFs<sup>47</sup> alter key parameters that affect ECM stiffness including density<sup>48</sup>, crosslinking<sup>4,49</sup>, and architectural and component changes<sup>50–52</sup>. Enhanced ECM density and rigidity facilitates liver and breast cancer detection via ultrasonography, and may indicate risk factors for tumour progression and therapeutic response<sup>53,54</sup>. ECM changes alter mechanotransduction<sup>55,56</sup> and promote malignant behaviour by disrupting epithelial morphogenesis<sup>57</sup>, growth factor secretion and signalling<sup>58</sup>, invasive phenotype<sup>59,60</sup> and stem cell differentiation<sup>61</sup>, as well as angiogenesis and vessel permeability<sup>62</sup>. As such, efforts have focused on characterizing altered ECM and how it contributes to tumour progression, with the goal of normalizing ECM for therapy<sup>3,63</sup> (FIG. 2). Studies applying physical and biological approaches *in vitro* and *in vivo*, combined with patient samples, have demonstrated that ECM stiffening promotes the progression of many cancers, including cancers of the breast, pancreas, brain, lung and skin<sup>64–66</sup>.

Traditionally considered independent risk factors, ECM stiffness and obesity were recently linked in the context of breast cancer<sup>67</sup>. Obesity-induced fibrotic remodelling of adipose tissue was previously shown to promote mammary tumour progression<sup>68</sup>. However, a multidisciplinary approach applying conformational fluorescence resonance energy transfer (FRET)-based ECM sensors, second-harmonic generation (SHG) ECM imaging, indentation-based mechanical measurements of ECM, combined with mouse models of

obesity showed that mammary fat pads from obese mice have increased numbers of myofibroblasts that deposit ECM, which is associated with enhanced stiffness and increased breast cancer cell growth<sup>67</sup>. Interestingly, caloric restriction in this mouse model reduced levels of  $\alpha$ -smooth muscle actin ( $\alpha$ -SMA), a myofibroblast marker, indicating that fibrosis and ECM can be normalized to enhance cancer therapy<sup>67</sup>.

Recently, ECM stiffening in PDAC was linked to tumour progression<sup>69</sup>. Elevated epithelial tumour cell signal transducer and activator of transcription 3 (STAT3) signalling via genetic perturbations in transforming growth factor- $\beta$  (TGF $\beta$ ) signalling induced stiff, matricellular-enriched fibrosis associated with altered collagen fibre structure, increased epithelial tension and shortened survival in a mouse model of PDAC. In addition to this change in tumour genotype affecting ECM stiffness, earlier work showed that sonic hedgehog (SHH) signalling by the stroma contributes to ECM stiffening<sup>70</sup>, and SHH inhibition reduced fibrosis and enhanced penetration of chemotherapeutic agents in mouse models of pancreatic cancer<sup>71</sup>. By contrast, recent work using SHH knockouts and ablation of activated stromal cells showed that complete abrogation of the desmoplastic response increases pancreatic cancer metastasis and reduces survival *in vivo*<sup>72,73</sup>.

As an alternative means to reprogramme the stroma, another recent study showed that the vitamin D receptor (VDR) is expressed on pancreatic stellate cells, and activation of VDR with the ligand calcipotriol reduced both inflammation and fibrosis in pancreatitis and human tumour stroma<sup>74</sup>. This was also associated with increased chemotherapeutic retention, reduced tumour volume and increased survival in mice. Collectively, recent findings indicate that the normalization and reprogramming of tumour stroma, rather than destruction, can improve PDAC treatment. Several molecules that normalize these stromal components, including vitamin D, hyaluronidase, and losartan, are being assessed in clinical trials, and some have shown promising outcomes (NCT01821729)<sup>6,45,46</sup>.

### Cancer glycocalyx

The sugar-rich glycocalyx coating on the surface of cancer cells (FIG. 3) facilitates tumour progression by enhancing angiogenesis, tumour growth and invasion<sup>75</sup>. The glycocalyx on epithelial and endothelial cells consists of proteoglycans and glycosaminoglycans, as well as matrix proteins including collagen<sup>76</sup>. Cell and matrix adhesion molecules are also embedded within the glycocalyx<sup>77</sup>. Mucin 1, a glycocalyx component that is overexpressed on cancer cells, mediates signal transduction to promote malignancy<sup>78</sup>. Hyaluronan, another glycocalyx component overexpressed on cancer cells, increases the tumorigenicity and metastatic potential of many cancers<sup>79</sup>. Anti-VEGF treatment can also increase hyaluronan in tumours in mice and patients and thereby confer treatment resistance<sup>80</sup>.

A recent interdisciplinary study using scanning angle interference microscopy, polymeric glycomimetics, FRET probes and mathematical modelling showed that glycocalyx physical properties can regulate tumour cell growth, survival and metastasis<sup>81</sup>. Expression of bulky glycoproteins in the cancer cell glycocalyx facilitated integrin clustering and membrane blebbing, which enhanced survival through alterations in MEK, PI3K, and focal adhesion kinase (FAK) signalling pathways. Circulating tumour cells (CTCs) from patient blood also

showed high surface expression of glycoproteins, suggesting that a bulky glycocalyx could promote tumour cell invasion and metastasis<sup>81</sup>.

The glycocalyx has also been implicated in mechanistic studies of immune evasion<sup>82,83</sup>. Increased expression of sialylated glycans on the cancer cell glycocalyx inhibited the activation of natural killer (NK) cells via engagement of inhibitory receptors on the NK cell surface<sup>82</sup>. Using glycopolymers functionalized with phospholipids on their ends, synthetically defined glycans were systematically introduced into the tumour cell membrane (FIG. 3) to probe the NK cell response<sup>82</sup>. Increased numbers of glycans reduced NK cell cytotoxicity in many tumour types, suggesting that glycocalyx sialylation offers a survival advantage to tumour cells under immunosurveillance. Approaches are now being explored for targeted removal of glycocalyx components to enhance NK cell-mediated tumour killing. For example, therapeutic conjugates consisting of the HER2-specific antibody trastuzumab fused to a recombinant sialidase removed sialylated glycans from tumour cells and induced potent NK cell cytotoxic activity<sup>84</sup>.

As engineers and physical scientists continue to study the TME, future efforts should increasingly focus on identifying safe and well-tolerated 'normalizing' therapeutics, which can be used in combination with immunotherapies, radiation or chemotherapies in the clinic. Such approaches hold great clinical promise, as some drugs that normalize the microenvironment are clinically approved for cancer and/or are being used in the clinic for other diseases<sup>6</sup>. The importance of the glycocalyx in cancer is only beginning to be recognized, and future detailed studies of its involvement in cancer will potentially lead to novel therapeutic strategies. For example, drugs that suppress the synthesis and/or assembly of the glycocalyx could be exploited for use in cancer therapy.

## Drug delivery

Delivery materials for dosage and/or spatiotemporally controlled drug release were pioneered in the 1970s<sup>85-87</sup>. Drug delivery systems offer a means to deliver therapeutics to malignant cells in a safe and targeted manner compared with standard treatments that rely on radiation and chemotherapy, which can kill normal cells and induce toxicity in patients<sup>88</sup>. These systems consist of a variety of soft (that is, polymers and lipids) and hard (inorganic) materials at the microscale and nanoscale, and they offer advantages for therapy including the improved delivery of poorly soluble agents, protection of molecules from harsh microenvironments, targeted delivery to cells and tissues, controlled release at precise dosages, and reduced toxicity<sup>89</sup>. Early work led to the first drug delivery technologies for cancer therapy, including matrix-type systems such as Gliadel (Eisai), which are implantable polymeric wafers for the treatment of brain tumours<sup>90</sup>, and Lupron depot (AbbVie), which are polymeric microspheres that release a hormone therapy for prostate cancer treatment<sup>91</sup>. At the nanoscale, the first liposome-encapsulated chemotherapeutic agent, a doxorubicin delivery system (Doxil; Janssen), has improved chemotherapy in the clinic by reducing patient cardiotoxicity<sup>92</sup>.

## Immunotherapy

One promising form of immunotherapy is the use of therapeutic cancer vaccines, which target tumours by mimicking immune mechanisms used against viral infections<sup>93</sup>. One major challenge is the delivery of vaccine antigens to lymph nodes, where much of the antitumour immune response is orchestrated<sup>94</sup>. Inspired by the ability of sentinel lymph node dyes used for biopsies to ‘hitchhike’ to serum albumin, lymph node-targeting amphiphilic vaccines were developed whereby an antigen or adjuvant is linked to a lipophilic albumin-binding tail using polymeric linkers<sup>95</sup>. Amphiphilic vaccines efficiently drained along with albumin into lymph nodes, induced a 30-fold increase in T cell priming and enhanced *in vivo* tumour cell killing while reducing systemic toxicity<sup>95</sup>. Biomaterial scaffolds can also be used as cancer vaccines and have been reviewed in detail<sup>93</sup>.

Nanoparticles have also garnered interest in immunotherapy, due to their ability to enhance delivery to target sites<sup>30</sup>. Nanoparticles targeting tumour-draining lymph nodes induced stronger immune and antitumour responses compared with targeting non-tumour-draining lymph nodes, possibly due to relief of immunosuppression and the boost of resident T cells that already had a high affinity for tumour-associated antigens<sup>96,97</sup>. In an alternative approach, mimicking pathogens in blood, nanoparticles containing tumour-derived RNA were engineered to systemically target dendritic cells, which initiate immune responses in lymphoid tissues in the presence of pathogens and foreign antigens<sup>98</sup> (FIG. 4). Without targeting ligands, nanoparticle surface charge was optimized via alterations in lipid:RNA ratios to enable delivery to dendritic cells in the spleen and lymphoid tissues. These nanoparticles enabled dendritic cells to translate tumour RNA and consequently to express tumour antigens, present them to T cells and prime an antitumour immune response. This approach is in clinical trials for melanoma therapy and has shown promising immune responses in patients (NCT02410733)<sup>98,99</sup>. Looking forward, nanoparticle systems to deliver replicon mRNA can be used to amplify antitumour immunity<sup>100</sup>.

The reinfusion of *ex vivo*-expanded immune cells into patients has also been used as a form of immunotherapy, as the first chimeric antigen receptor (CAR) T cell gene therapy, Kymriah (Novartis), was recently approved by the US Food and Drug Administration (FDA) for the treatment of certain paediatric and young patients with a form of acute lymphoblastic leukaemia. However, adoptive T cell therapies require high systemic dosing of toxic adjuvant drugs<sup>101</sup>. To overcome this high dosing, the surfaces of immune cells have been functionalized with adjuvant-loaded nanoparticles via chemical conjugation, which enhances the antitumour response of T cells while minimizing systemic toxicity<sup>102</sup>. Engineering the immune cell surface with nanoparticles containing immunomodulators can also regulate the T cell synapse and antitumour immunity<sup>103</sup>. A similar approach has also been used to functionalize T cells with chemotherapeutic-containing nanoparticles, which actively targeted lymphoma in lymph nodes in which tumours typically evade systemic therapies<sup>104</sup>.

As an alternative to *ex vivo* approaches, strategies have been developed to bind therapeutics to immune cells in the bloodstream<sup>105,106</sup>. Inspired by NK cell cytotoxic activity, liposomal systems functionalized with a cell adhesion receptor, E-selectin, and an immune cytokine, tumour necrosis factor-related apoptosis-inducing ligand (TRAIL, also known as TNFSF10),

that binds to death receptors on cancer cells to trigger apoptosis<sup>107</sup> have been developed to tether to immune cells in the circulation<sup>105</sup>. In mice, this approach improved the circulation half-life of TRAIL, killed tumour cells in the bloodstream and prevented the spontaneous metastasis of prostate cancer<sup>108</sup>.

### RNAi delivery systems

RNAi has the potential to efficiently silence ‘undruggable’ genes that contribute to disease progression. The most advanced RNAi-based drug to date is a lipid nanoparticle RNAi drug, patisiran, developed by Alnylam Pharmaceuticals, which has successfully met its primary efficacy end point and all secondary end points in a recent phase III clinical trial; it inhibits hepatic production of transthyretin as a form of transthyretin amyloidosis therapy (NCT01960348)<sup>109,110</sup>. In oncology, several early-phase trials of small interfering RNA (siRNA) therapeutics for solid cancers are ongoing or have been completed (NCT00938574; NCT01591356)<sup>109,111–113</sup>. Improvements in RNAi-based therapeutics are still needed, with a challenge being the safe and efficient delivery of siRNA to tumours *in vivo*. Nanoparticles as non-viral delivery vectors can address these needs by preventing nucleic acid degradation, evading immune detection, avoiding renal clearance and mediating cell entry and endosomal escape<sup>114</sup> (FIG. 5).

Recently, nanoparticles consisting of a cationic lipid–siRNA complex-containing poly(D,L-lactide-co-glycolide) (PLGA) polymer core and a lipid-polyethylene glycol (PEG) shell extended the circulation half-life of systemically administered siRNA to ~8 hours, compared with naked siRNA, which rapidly clears from blood within 30 min, with high accumulation in tumours and effective gene silencing *in vivo*<sup>115</sup>. Prohibitin, a protein associated with drug resistance that is upregulated in several cancers and lacks effective inhibitors, was silenced by RNAi nanoparticle delivery and shown to inhibit tumour growth in a mouse model of NSCLC<sup>115</sup>. In addition to enhancing biodistribution, siRNA delivery vehicles have been designed to improve tumour penetration, through the use of tandem peptides capable of both tumour homing and penetration along with siRNA delivery across cell membranes<sup>116</sup>. The peptides were electrostatically bound to siRNA to form nanoparticles, and they effectively silenced the oncogenic inhibitor of DNA binding 4 (*Id4*), suppressing the growth of ovarian cancer xenografts and extending survival in mice<sup>116</sup>. siRNA delivery to the brain and endothelium has also been demonstrated using nanoparticles. Spherical nucleic acid (SNA) nanoparticles, consisting of gold nanoparticles covalently functionalized with densely packed siRNA duplexes, were engineered for the treatment of glioblastoma<sup>117</sup>. In a process dependent on the activity of scavenger receptors, SNAs penetrated the blood–brain and blood–tumour barriers to reduce glioma progression in a xenograft mouse model<sup>117</sup>. Beyond the brain, nanoparticles that induce potent gene silencing in endothelium were discovered through systematic screening of a combinatorial chemical library of ~2,400 formulations<sup>118</sup>. Nanoparticles consisting of low-molecular-weight polyamines and lipids preferentially delivered siRNA to endothelium in many organs *in vivo* without significantly reducing gene expression in liver and immune cells<sup>118</sup>. In a model of metastatic Lewis lung carcinoma, silencing of angiogenesis regulators reduced primary tumour growth and lung surface metastases *in vivo*<sup>118</sup>. The mechanism of endothelium targeting remains unclear, but it likely involves nanoparticle–serum protein interactions that enhance delivery<sup>119</sup>. Similar



nanoparticle formulations combining both siRNA and microRNA (miRNA) have also been used to treat genetically engineered mouse models of lung cancer that have not shown durable responses to chemotherapy<sup>120</sup>. Other recent nanoparticle delivery systems have been engineered to co-deliver siRNA and chemotherapies via layer-by-layer self-assembly<sup>121</sup> and to encapsulate siRNA within materials that have intrinsic cytotoxic effects toward tumour cells<sup>122</sup>.

### Implantable delivery devices

The ability to predict and execute cancer therapeutic regimens remains an unmet need, owing to a failure to identify optimal drug choices to treat a patient's tumour and the development of drug resistance over time, even when the optimal therapy is initially administered<sup>123</sup>. These factors remain challenging due to a lack of methods to screen the responses of a patient to a range of drugs *in vivo*. Recently, implantable devices have been engineered to administer drugs directly into tumours in mice *in situ*<sup>124,125</sup>. The devices deliver small doses of drugs simultaneously within the tumour, after which cytotoxic effects are assessed (FIG. 6). In one example, a cylindrical, microscale implantable device was fabricated from medical-grade Delrin acetal resin blocks with 16 separate drug reservoirs<sup>124</sup>. These devices were implanted into tumours using a biopsy needle, and they released microdoses of drugs into spatially distinct tumour regions. Small samples of the surrounding tissue and the device were removed via a standard biopsy procedure and showed correlations between apoptosis and the administered drug concentration from the device<sup>124</sup>. The cell death response to drugs delivered from the device was comparable to that of conventional systemic delivery, demonstrating that the device mimics the effects of systemic administration.

Another device consisting of an array of six micro-needles was developed to microinject drugs into mouse tumours<sup>125</sup> (FIG. 6). The needles inject a 6 mm drug microtrack within the tumour, which is then excised and analysed for drug efficacy. The device predicted responses to systemically delivered drugs in mice, and it determined both drug resistance and unexpected sensitivity to cyclophosphamide in multidrug-resistant lymphomas. The device has moved into clinical testing, delivering microinjections of drugs into canines and human patients while remaining well tolerated (NCT01831505 and NCT03056599)<sup>125–127</sup>. Collectively, this class of devices offers personalized drug assessment *in vivo* to tailor patient therapies.

Despite advances in drug delivery, unmet clinical challenges remain. The development of novel biologics will require advanced delivery systems that protect these therapeutics in the body. For patients who fail to adhere to daily dosing regimens, devices that release drugs over weeks and months within the body will be needed to improve responses to therapies. Gene editing technologies, such as CRISPR–Cas9, zinc-finger nucleases and transcription activator-like effector nucleases, have the potential to enable permanent genetic modifications in diseased cells that contribute to cancer and will require new systems that efficiently deliver a combination of proteins, small RNAs, and/or mRNAs into target cells<sup>128</sup>.

## Cellular and molecular imaging

### Imaging biomarkers

Quantifying biomarkers is essential for basic cancer research, clinical diagnosis, early detection, and mapping disease severity<sup>129,130</sup>. One standard quantification technique, immunohistochemistry, is limited to detecting one or two biomarkers in samples because of spectral and spatial overlap constraints<sup>131</sup>. Recently, a method termed multiplexed ion beam imaging has been developed to expand the detection of biomarkers by staining tissues and cells with antibodies carrying isotopically pure elemental metal reporters<sup>132,133</sup> (FIG. 7). Secondary ion mass spectrometry is then used to detect secondary ions released from metal-tagged antibodies, thereby producing images of the spatial features of molecular expression within tissues<sup>132</sup>. In comparison to fluorescence-based methods, this technique is capable of analysing up to 100 metal-tagged targets simultaneously and was shown to detect ten labels in formalin-fixed, paraffin-embedded human breast tumour tissue sections<sup>132</sup>. In theory, this method could also be applied to fresh samples of tumour tissue.

*In vivo* imaging of biomarkers is essential for assessing tumours in organs not readily biopsied, including the brain. Brain tumours are typically characterized by genetic abnormalities that are difficult to detect *in vivo*<sup>134</sup>. Recently, noninvasive detection of 2-hydroxyglutarate (2HG), a metabolite associated with isocitrate dehydrogenase (IDH)-mutated gliomas in patients, was demonstrated using proton magnetic resonance spectroscopy (MRS)<sup>135</sup>. MRS measures high concentrations of metabolites in tissues via MRI<sup>135</sup>. Using MRS, concentrations of 2HG in 30 patients with glioma were estimated and correlated with IDH mutations<sup>135</sup>. Given that MRI is the primary modality for clinical evaluation of patients with glioma, 2HG detection could have important implications in the diagnosis, prognosis and stratification of brain tumours.

Novel molecular imaging probes are also being developed by engineers to enable tumour detection deep within tissues using modalities including MRI and photoacoustic imaging<sup>136</sup>. Photoacoustic imaging has translated rapidly to the clinic for many cancer applications, in part owing to this type of imaging being able to provide information via endogenous chromophores such as oxy- and deoxyhaemoglobin<sup>136</sup>. As not all cancers provide sufficient endogenous contrast to exploit photoacoustic imaging, contrast agents have been engineered to produce a photoacoustic signal high enough to be detected even at low concentrations, while being able to target diseased tissues. Gold nanorods and single-walled carbon nanotubes, which possess a sufficiently large optical absorption cross section to maximize the photoacoustic signal of the imaging probe while being small enough to be eliminated from the body, have improved photoacoustic imaging of cancer in mice<sup>137,138</sup>. Nanoparticles have also been engineered to be exploited in photoacoustic imaging to delineate the margins of brain tumours and map lymph nodes in mice<sup>139,140</sup>. Beyond photoacoustic imaging, novel probes are being developed for MRI. When targeting tumours using MRI, conventional ligand-targeted imaging probes typically fail to deliver sufficient numbers of magnetic nanoparticles for image contrast<sup>141–143</sup>. To increase the number of nanoparticles delivered to tumours per targeting ligand and hence improve contrast, bacteriophages have been used as scaffolds to display nanoparticles and targeting ligands for tumour imaging via MRI in

mice<sup>144</sup>. While novel probes can impact diagnosis and surgical interventions at earlier stages of cancer, it is important to note that such agents add considerable cost to imaging exams, and new agents could require lengthy FDA approval processes.

### Imaging therapeutic delivery

Imaging is playing an increasingly important role in drug development, clinical trial design and enhancing the delivery and monitoring of therapies<sup>145</sup>. For example, positron emission tomography (PET) imaging in the clinic can guide tumour biopsies, deliver drugs via image guidance, and detect therapeutic response in the absence of tumour shrinkage<sup>129,146</sup>. In research settings, intravital microscopy is used to study drug pharmacokinetics and pharmacodynamics using fluorescent companion imaging drugs<sup>147–149</sup>, combined with imaging of orthotopic tumour xenograft mouse models and methods to study drug targeting<sup>150</sup>. For example, precursor compounds have been conjugated to small, cell-permeable fluorophores to synthesize therapeutically active fluorescent companion imaging drugs<sup>147</sup>. Through the use of an implanted window chamber or medial skin incision at the tumour site, *in vivo* microscopy has enabled the detection of companion imaging drugs in orthotopic tumours with subcellular resolution and frame rates of several seconds<sup>147</sup>. These advances enable fundamental understanding of drug behaviour *in vivo* and provide critical insight into predicting drug efficacy. These techniques provide numerous advantages over the conventional study of therapeutic mechanisms in cell culture, which does not provide insight into delivery and whether or not the assumed mechanism of drug action occurs *in vivo*.

Imaging techniques have recently been developed to quantify drug concentrations inside cellular compartments and the uptake of drugs within tumour cell populations, as well as to determine the spatiotemporal dynamics of tumour drug resistance<sup>148</sup>. A combination of intravital imaging and automated single-cell tracking identified a new therapeutic mechanism of action for eribulin, an FDA-approved cytotoxic agent that inhibits microtubule growth<sup>148</sup>; intravital imaging showed that drug accumulation depended on drug efflux mediated by multidrug resistance 1 (MDR1, also known as ABCB1) and on tumour vascular architecture<sup>148</sup>, a mechanism that likely would have not been identified in the absence of *in vivo* imaging<sup>148</sup>. Using *in vivo* single-cell imaging in tumour-bearing mice, another recent study showed that polymeric nanoparticle encapsulation of a fluorescent platinum (IV) pro-drug affected both drug pharmacokinetics and drug uptake and response<sup>147,151</sup>. Intravital imaging showed high accumulation of nanoparticles within tumour-associated macrophages (TAMs), which then released drug to neighbouring tumour cells over time, implicating macrophages as slow release depots of drugs<sup>151</sup>.

Pairing MRI and intravital imaging can be used to identify tumours with a higher likelihood of nanoparticle accumulation<sup>152</sup>. To identify tumours with optimal EPR characteristics, magnetic nanoparticles 30 nm in diameter were used to predict colocalization of therapeutic nanoparticles via MRI. Mice with the highest magnetic nanoparticle intratumoural accumulation detected via MRI also showed the highest fluorescent therapeutic nanoparticle accumulation via intravital imaging. These mice showed the greatest reduction in tumour volume when subsequently treated with a paclitaxel-encapsulated nanoparticle<sup>152</sup>. Given

that magnetic nanoparticles such as Ferumoxytol (AMAG Pharmaceuticals) are FDA-approved for other applications<sup>153</sup>, this approach has potential to select patients with high EPR characteristics and most likely to be responsive to nanoparticle-delivered therapies.

### Cancer cell invasion and metastasis

Intravital imaging in animals has revealed aspects of cancer cell invasion and metastasis that cannot be quantified via genetic studies or tumour biopsies<sup>20,154</sup>. Confocal and multiphoton microscopy can be used to characterize tumour and immune cell behaviour in the microenvironment through fluorescent mouse models<sup>154,155</sup>. Parameters including cell migration mode, cell velocity and the number of migrating cells, along with tumour stroma–vessel interactions, can be quantified<sup>156</sup>. In particular, intravital imaging has shown that macrophage interactions with tumour cells promote tumour cell invasion and metastasis<sup>157,158</sup>. More specifically, *in vivo* imaging showed that breast cancer cell subpopulations migrate together with macrophages towards vessels in response to paracrine chemotactic signalling<sup>159</sup> and intravasate at sites enriched with macrophages<sup>158,160</sup>. In a mouse model of breast cancer, colony-stimulating factor 1 receptor (CSF1R) antibodies administered via intraperitoneal injection depleted TAMs and dendritic cells, which delayed tumour growth, reduced vascularity and decreased lung metastasis. However, blocking the CSF1 pathway can have adverse effects on tumour progression with some tumour types, as CSF1 blockade significantly reduced the survival benefit of a dual cediranib (a pan-VEGFR tyrosine kinase inhibitor) and MEDI3617 (an angiopoietin 2 neutralizing antibody) therapy in a mouse glioblastoma model<sup>161</sup>. In addition, intravital imaging of mouse mammary tumours with MMPsense, a fluorescent probe for the activity of matrix metalloproteinases (MMPs) 2, 3, 7, 9 and 13 showed that TAMs and dendritic cells possess substantial MMP activity, which promotes invasion<sup>158</sup>.

Metastatic cancer cells that migrate towards blood and lymphatic vessels can cross ECM barriers via collagen network remodelling<sup>162</sup>. Advances in SHG and third-harmonic generation (THG) microscopy enable noninvasive imaging of collagen remodelling *in vitro* and *in vivo* without exogenous labelling of collagen<sup>162,163</sup>. SHG results when two photons with the same frequency interact with one nonlinear material to create one photon of half the wavelength and is typically elicited by collagen fibres in interstitial tissues<sup>163</sup>. THG results when three simultaneously arriving photons combine to make one of triple the frequency of an individual photon, making it ideal for detecting water–lipid and water–protein interfaces, including cellular membranes and tissue discontinuities along blood and lymph vessels<sup>65</sup>. In the clinic, SHG is used to classify collagen alignment in biopsied tissue sections from patients with cancer, and it has shown potential in predicting breast cancer survival<sup>164</sup>. SHG and THG provide minimal photodamage, enhanced optical penetration and quantitative information on collagen remodelling<sup>165</sup>. Combining SHG and THG with fluorescence microscopy provides insight into tumour tissue organization, cell–matrix interactions, blood flow dynamics, and the dissemination of microvesicles<sup>65,166</sup>. More specifically, the combination of all three imaging platforms enabled tracking of melanoma invasion into the dermis ~600 µm deep, along with reconstruction of the tumour cell invasion mode and tissue tracks to determine the invasion routes and outcome<sup>65</sup>. Differential forms of cancer cell invasion and migration were identified, as cancer cells invaded in a collective manner in pre-

existing spaces along the interfaces of collagen bundles, whereas discontinuous collagen-rich stroma supported the dissemination of single tumour cells<sup>65,167</sup>.

Looking forward, physical scientists must address the challenge of detecting small tumours (that is, <1 mm<sup>3</sup>) deep within tissues to improve patient outcome. Single-cell imaging techniques that reach beyond current depth limits (that is, ~500 µm), with increased multiplexing (that is, >10 targets imaged simultaneously) are needed to study cancer at the molecular level. A novel class of quantum dots that emit in the short-wave infrared region (SWIR; 1000–2000 nm), where large organisms are rendered translucent for fluorescence imaging<sup>168</sup>, may also become invaluable in the fundamental understanding and treatment of cancer. Improved features of this imaging technique include a lack of autofluorescence, low light absorption by blood and tissue, and reduced scattering. Super-resolution ultrasound imaging, which goes beyond the sub-millimetre resolution of clinical ultrasound imaging by imaging at ultrasound frame rates, now enables noninvasive whole-organ mapping of microvasculature *in vivo*<sup>169</sup>. Additionally, novel techniques based on MRI, such as hyperpolarized <sup>13</sup>C MRI and chemical exchange saturation transfer (CEST), hold potential for noninvasive imaging of tumour location and metabolism over time to improve both initial diagnosis and monitoring therapy<sup>170,171</sup>.

## Microfluidics and microfabrication

### In vitro models of migration and mechanotransduction

The mechanisms behind metastasis remain elusive, despite the fact that it contributes to more than 90% of cancer-related deaths<sup>167</sup>. The small degree of insight into tumour cell migration during metastasis is partially a reflection of the lack of *in vitro* models that recapitulate the process. Early models incorporating physiological fluid flow led to the discovery of autologous chemotaxis, a mechanism of tumour cell migration and homing to lymphatics<sup>17,172</sup>. More recent studies have used microfluidics to study the effects of interstitial flow on tumour cell migration; a microfluidic device comprising a region containing single cells suspended in collagen separating two microfluidic channels<sup>173</sup> provided further evidence for autologous chemotaxis along with a competing mechanism whereby tumour cells migrate against the direction of interstitial flow.

In addition to fluid flow, microfabricated models are used to study tumour cell migration through confined microenvironments<sup>174,175</sup>. One migration process that can be modelled is the track-like structures in ECM used for *in vivo* tumour cell migration, which can be both naturally occurring and generated by cell–ECM remodelling through secretion of MMPs<sup>176</sup>. Using micromoulding technology, collagen microtracks were fabricated that mimic those generated by proteolytically active cancer cells *in vivo*<sup>177,178</sup>. These microtracks enabled migration of cells that cannot invade 3D collagen matrices, enhanced motility, and revealed that microtrack migration can occur in the absence of MMPs<sup>177</sup>. Microtracks substantially reduced tumour cell traction force generation, matrix remodelling and deformation processes necessary for tumour cell migration through matrices<sup>178</sup>.

Beyond microtracks, *in vitro* models have been developed to study tumour invasion where matrix stiffness and channel width can be altered independently<sup>179</sup>. The approach combines

the polymerization and gelation of polyacrylamide hydrogels of tuneable stiffness onto silicon micromoulds to create microchannels of defined stiffness and geometry. Tumour cells were shown to migrate faster in narrow channels compared with wider ones at a given stiffness, while physical confinement increased migration speed with increasing ECM stiffness<sup>179</sup>. Cellular traction polarization was essential to this response, as inhibition of non-muscle myosin II dissipated polarization and rendered the relationship between migration and ECM stiffness less sensitive to confinement. Models of confinement have also identified tumour cell migration mechanisms dependent on both cell-volume regulation and water permeation, where water and ions flow in through the leading edge and out from the trailing edge of the cell<sup>180</sup>. Using microfabricated constrictions of varying dimensions, the size and mechanical properties of the tumour cell nucleus were found to be essential to migration<sup>181–184</sup>. Constrictions below a threshold cross-sectional area increased nuclear envelope rupture of tumour cells as they migrated through the confined space. However, these nuclear envelope ruptures were temporary, as endosomal sorting complex machinery was recruited to reseal the nuclear membrane, ensuring cell viability after migration through tight restrictions<sup>181,182</sup>.

### Organs-on-chips

‘Organs-on-chips’ are microfabricated devices containing cells and tissues, which are organized to mimic organ-level functions<sup>15</sup>. These devices recreate physiological functions not possible using traditional 2D and 3D systems, including tissue–tissue interfaces, physicochemical cues and microenvironments, and blood vessel perfusion. Real-time, high-resolution imaging of tissues, along with analysis of cellular biochemical, genetic and metabolic activity can be quantified<sup>185</sup>. These systems can advance the screening and validation of cancer therapeutic agents, their mechanisms of action, and toxicity testing<sup>185</sup>.

Compartmental microfluidic models of endothelium have been developed for region-specific activation of endothelial cells under physiological flow, to identify vessel drug targets for breast cancer metastasis not previously identified in 2D culture<sup>186</sup>. Increased complexity and clinical relevance can be incorporated into such systems, as devices have been developed to mimic interactions between CTCs, endothelium and bone microenvironments as a model of metastasis to bone<sup>187</sup>. This system recapitulated CTC transendothelial migration and tumour formation in bone tissue *in vitro*, detected via real-time microscopy. The model identified C-X-C chemokine receptor 2 (CXCR2) on CTCs and C-X-C chemokine ligand 5 (CXCL5) secreted by osteo-differentiated bone marrow-derived mesenchymal stem cells (MSCs) as major signalling mediators in the extravasation process, implicating both as therapeutic targets for metastasis<sup>187</sup>.

To mimic the pharmacokinetics and pharmacodynamics of drugs in humans, ‘body-on-chip’ systems consisting of interconnected, compartmentalized tissues representing the human body have been developed<sup>16</sup> (FIG. 8). A multi-organ model of interconnected microchambers representing colon cancer, liver, and bone marrow was able to reproduce the *in vivo* metabolism of a chemotherapeutic pro-drug of 5-fluorouracil (5-FU), tegafur, into 5-FU in the liver<sup>188</sup>. The model also reproduced tumour death by 5-FU, which was not

observed in static culture<sup>188</sup>. Furthermore, these models have also been linked with computational pharmacokinetics and pharmacodynamics to improve drug predictability<sup>189</sup>.

### CTC and exosome isolation

CTCs shed by tumours into the bloodstream are being utilized for detection of metastatic cancer<sup>190</sup>. As a therapeutic tool, CTCs are used to monitor the appearance of drug-resistant mutations, and they can be cultured *ex vivo* for personalized testing of drugs<sup>191</sup>. The use of CTCs in the clinic for prognosis and diagnosis is complicated by lengthy procedures for their isolation from patient blood, resulting in impurities and low yields<sup>190</sup>. The use of microfluidics has improved CTC isolation by exploiting biological (that is, target antigens) and physical properties (that is, fluid flow, cell size, shape, density and deformity) to separate rare CTCs from billions of contaminating blood cells<sup>192</sup>. First-generation devices utilized microfluidics containing microposts functionalized with antigens to capture CTCs, while non-target blood cells perfused through the device<sup>193</sup>. Nanostructures and microstructures have since been developed with additional immuno-based capture markers to improve CTC purity<sup>194,195</sup>. Given that CTCs are heterogeneous and might not express conventional epithelial biomarkers, devices have been developed for negative selection, where white blood cells are captured while CTCs are isolated via perfusion<sup>196</sup>. Given that CTC clusters have shown greater metastatic potential than singular CTCs and are associated with poor prognosis<sup>197–199</sup>, microfluidics have now been engineered to trap CTC clusters through the use of rows of triangular microposts<sup>200</sup> (FIG. 8).

Exosomes ~30–100 nm in size are another source of biomarkers secreted in large amounts during carcinogenesis, and they carry proteins and miRNAs associated with metastatic tumours<sup>201</sup>. Exosome isolation is hampered by time-consuming ultracentrifugation steps and results in low yields (5–25%)<sup>202</sup>. To overcome these obstacles, microfluidics have also been used for exosome isolation, through incorporation of herringbone grooves within the microchannels to promote exosome mixing, and a channel surface functionalized with antibodies to capture exosomes<sup>203</sup>. Microfluidics have also been integrated with antibody-functionalized nanoplasmonic exosome sensors, in which surface plasmon resonance is utilized via periodic nanohole arrays on a metal film to detect and identify exosomes from patients with ovarian cancer based on surface protein expression<sup>204</sup> (FIG. 8). Similar to CTC isolation, deterministic lateral displacement pillar arrays have been fabricated at the nanoscale to induce size-based displacement and fractioning of exosomes<sup>205</sup>.

Looking forward, microfabrication and microfluidics in cancer research will require the development of novel materials to enable mass production, along with reductions in the complexity of the experimental setup. Both improvements will provide opportunities for the widespread use of cancer tissue models and early detection (that is, exosomes, CTCs and circulating tumour DNA (ctDNA)) devices in research laboratories and the clinic. Tissue models should be validated with animal and clinical trial data to determine whether human physiology can be fully mimicked and whether they can be predictive of therapy. These systems must be robust and reproducible to be adopted by pharmaceutical companies for drug discovery. CTC isolation devices will likely be most useful for later-stage cancers

where sufficient CTCs are detectable. Exosome isolation devices can potentially be used as a preventive-based measure before metastasis, as exosomes are present in measurable levels in blood before metastatic dissemination.

## Future directions

The integration of engineering, physical sciences, and oncology over the past 50 years has proved to be a powerful approach to cancer research, leading to medical and technological breakthroughs. Looking forward, integration of these disciplines has the potential to enhance early diagnosis of cancer, which will save on expensive later-stage and last-minute treatments of metastatic cancer. The effectiveness of treatments can also be increased using such approaches, including novel delivery vehicles for immunotherapies and vaccines to enable our own bodies to fight cancer. Medical devices developed by engineers can be implanted into the tumours in a minimally invasive manner, which can better predict the efficacy of drugs *in vivo* and dramatically save on the costs of therapeutics. In terms of fundamental understanding of cancer, convergence of these disciplines will lead to new computational models of complex cancer systems, advanced imaging modalities from the subcellular to the whole-body level, and single-cell analyses with detailed protein, RNA and DNA characterization to expand our understanding of what drives cancer progression.

To fully realize the promise of engineering and physical sciences in oncology, funding from federal agencies should be specifically targeted towards research at the intersection of these disciplines. Indeed, in the US, the National Cancer Institute (NCI) has launched several programmes over the past two decades to catalyse such research, including the Alliance for Nanotechnology in Cancer in 2004, where experts in nanotechnology have worked side by side with oncologists and clinicians to foster new approaches in cancer detection and treatment<sup>206</sup>. More recently, in 2009, the NCI also launched the Physical Sciences–Oncology Center (PS–OC) Network of 12 interdisciplinary teams, with the goal of incorporating the perspectives of physical scientists that might formulate and approach problems in a distinct way that provides complementary insights into cancer<sup>207</sup>. In 2015, the NCI continued into phase II of the Physical Sciences–Oncology initiative by building a collaborative network of ten PS–OCs and eight Physical Sciences–Oncology Projects (PS–OPs). In addition to programs at the NCI, the National Institutes of Health (NIH), National Science Foundation (NSF), the US Department of Defense, and the US Department of Energy are now involved in some aspects of research at the integration of physical sciences, engineering and the life sciences — broadly referred to as convergence research<sup>208</sup>. However, the level of support for convergence research is small, with only 3% of all NIH funding going to principal investigators in physical sciences, engineering and mathematics<sup>208</sup> and less going to those focused on integrating their expertise into cancer research.

In the future, engineering and physical sciences in oncology research cannot rely only on special funding programmes but will require dedicated strategic and funding plans from agencies across the world to achieve its full potential. Such dedicated funding mechanisms will enable engineers and physical scientists to collaborate with clinicians and biologists at the earliest stages of research, where the greatest impact in our understanding of the



physical, genetic and biochemical properties of cancer can be made. Advances at the interface of these disciplines will supply the innovations that will give physicians and patients the diagnostics, information and therapeutics to eliminate the disease.

## Acknowledgments

This work was supported in part by a Cancer Center Support (core) Grant P30-CA14051 from the National Cancer Institute and a grant from the Koch Institute's Marble Centre for Cancer Nanomedicine (to R.L.) and the National Cancer Institute (P01-CA080124, R01-CA126642, R01-CA115767, R01-CA096915, R01-CA085140, R01-CA098706) and NCI Outstanding Investigator Award (R35-CA197743) (to R.K.J.). M.J.M. was supported by a Burroughs Wellcome Fund Career Award at the Scientific Interface, an NIH F32 fellowship (award number CA200351) and a grant from the Burroughs Wellcome Fund (no. 1015145). The authors thank V. Chauhan, M. Oberli, K. Kozielski, K. Wang, B. R. Seo, D. Fukumura, L. Munn and T. Stylianopoulos for helpful discussions and feedback on the manuscript. The authors thank K. Wang for assisting with conceptualization of figures.

## Glossary

### **Tumour microenvironment (TME)**

The microenvironment surrounding cancer cells, which is composed of blood and lymphatic vessels, fibroblasts, immune cells and other non-malignant host cells, all embedded within extracellular matrix.

### **Interstitial fluid pressure (IFP)**

Pressure exerted by free interstitial tissue fluid. Increased IFP in tumours pushes fluid, growth factors, administered therapeutic molecules and cells to the peri-tumour tissue, aiding tumour progression.

### **Enhanced permeability and retention (EPR)**

An effect based on proposed mechanisms for selective tumour delivery of drugs. These mechanisms include the greater permeability of tumour vessels than normal vessels to macromolecules and the retention of macromolecules in tumours due to poor lymphatic clearance.

### **Computed tomography (CT)**

A diagnostic imaging test used to create images of internal organs, bones, soft tissue and blood vessels. In oncology, cross-sectional CT images are used to confirm the location and size of tumours.

### **Solid stresses**

Stresses exerted by and accumulated within solid components of tissues (that is, cells and extracellular matrix) during growth and progression. In tumours, solid stress is elevated due to growth and is independent of high interstitial fluid pressure.

### **Tumour deformation assays**

An assay to quantify stress in tumours. Excised tumours are cut in the middle of the tumour, and stress relaxation is quantified as the extent of tumour opening normalized to the diameter of the tumour.

### **Desmoplasia**

The formation and growth of fibrous tissue. In cancer, desmoplasia may occur around a neoplasm, causing dense fibrosis around the tumour.

**Ultrasonography**

A technique using echoes of ultrasound pulses to delineate objects or areas of different density in the body. In cancer, ultrasonography is used to detect solid tumours.

**Matricellular-enriched fibrosis**

The thickening and scarring of tissue surrounding a tumour, composed of dynamically expressed, non-structural proteins that are present in the extracellular matrix.

**Hyaluronidase**

An enzyme that catalyses the degradation of hyaluronic acid, a component of the extracellular matrix that contributes to tumour growth.

**Adjuvant**

A substance that enhances the body's immune response to foreign antigens.

**Replicon mRNA**

A self-replicating nucleic acid that amplifies production of the encoded protein and prolongs translation.

**Scavenger receptors**

A group of receptors that recognize low-density lipoprotein that has been modified by oxidation or acetylation.

**Microdoses**

Doses of a drug on the microgram scale, or about one-millionth of the systemic dose of a drug, that are intended to produce a beneficial result while avoiding undesirable side effects.

**Bacteriophages**

Long, tubular viruses that infect specific bacteria; they have been used as scaffolds for nanoparticles and targeting ligands for imaging tumours using magnetic resonance imaging (MRI)

**Autologous chemotaxis**

A mechanism by which a tumour cell can receive directional cues while at the same time being the source of such cues, enabling dissemination into the lymphatic system.

**Surface plasmon resonance**

An optical technique for detecting the interaction of two different molecules or particles, in which one is mobile and one is fixed on a thin gold film.

**Deterministic lateral displacement pillar arrays**

Arrays of pillars fabricated from silicon used to sort, separate and enrich microscale particles including parasites, bacteria, blood cells and tumour cells under flow conditions.

## References

1. Jain RK, Martin JD, Stylianopoulos T. The role of mechanical forces in tumor growth and therapy. *Annu. Rev. Biomed. Eng.* 2014; 16:321–346. Comprehensive review of the role of physical forces in tumour progression and therapy for those new to the fields of engineering and physical sciences in oncology. [PubMed: 25014786]
2. Wirtz D, Konstantopoulos K, Searson PC. The physics of cancer: the role of physical interactions and mechanical forces in metastasis. *Nat. Rev. Cancer.* 2011; 11:512–522. [PubMed: 21701513]
3. Lu P, Weaver VM, Werb Z. The extracellular matrix: a dynamic niche in cancer progression. *J. Cell Biol.* 2012; 196:395–406. [PubMed: 22351925]
4. Tse JM, et al. Mechanical compression drives cancer cells toward invasive phenotype. *Proc. Natl Acad. Sci. USA.* 2012; 109:911–916. [PubMed: 22203958]
5. Jain RK. Antiangiogenesis strategies revisited: from starving tumors to alleviating hypoxia. *Cancer Cell.* 2014; 26:605–622. [PubMed: 25517747]
6. Jain RK. Normalizing tumor microenvironment to treat cancer: bench to bedside to biomarkers. *J. Clin. Oncol.* 2013; 31:2205–2218. [PubMed: 23669226]
7. Mitchell MJ, King MR. Computational and experimental models of cancer cell response to fluid shear stress. *Frontiers Oncol.* 2013; 3:44.
8. DeVita VT, Chu EA. History of cancer chemotherapy. *Cancer Res.* 2008; 68:8643–8653. [PubMed: 18974103]
9. Verellen D, et al. Innovations in image-guided radiotherapy. *Nat. Rev. Cancer.* 2007; 7:949–960. [PubMed: 18034185]
10. Winkler F, et al. Kinetics of vascular normalization by VEGFR2 blockade governs brain tumor response to radiation: role of oxygenation, angiopoietin-1, and matrix metalloproteinases. *Cancer Cell.* 2004; 6:553–563. Seminal study revealing the molecular and physiological mechanisms of vascular normalization, along with how normalization improves the outcome of various therapies. [PubMed: 15607960]
11. Wong C, et al. Multistage nanoparticle delivery system for deep penetration into tumor tissue. *Proc. Natl Acad. Sci. USA.* 2011; 108:2426–2431. [PubMed: 21245339]
12. Jain RK. An indirect way to tame cancer. *Scientif. Am.* 2014; 310:46–53.
13. Jain RK, Stylianopoulos T. Delivering nanomedicine to solid tumors. *Nat. Rev. Clin. Oncol.* 2010; 7:653–664. [PubMed: 20838415]
14. Chauhan VP, et al. Normalization of tumour blood vessels improves the delivery of nanomedicines in a size-dependent manner. *Nat. Nanotechnol.* 2012; 7:383–388. First study demonstrating that normalization of leaky, disordered tumour vasculature enhances the delivery of smaller nanoparticle therapeutics to tumours. [PubMed: 22484912]
15. Bhatia SN, Ingber DE. Microfluidic organs-on-chips. *Nat. Biotechnol.* 2014; 32:760–772. [PubMed: 25093883]
16. Esch MB, King TL, Shuler ML. The role of body-on-a-chip devices in drug and toxicity studies. *Annu. Rev. Biomed. Eng.* 2011; 13:55–72. [PubMed: 21513459]
17. Swartz MA, Lund AW. Lymphatic and interstitial flow in the tumour microenvironment: linking mechanobiology with immunity. *Nat. Rev. Cancer.* 2012; 12:210–219. [PubMed: 22362216]
18. Hanahan D, Coussens LM. Accessories to the crime: functions of cells recruited to the tumor microenvironment. *Cancer Cell.* 2012; 21:309–322. [PubMed: 22439926]
19. Gajewski TF, Schreiber H, Fu Y-X. Innate and adaptive immune cells in the tumor microenvironment. *Nat. Immunol.* 2013; 14:1014–1022. [PubMed: 24048123]
20. Jain RK, Munn LL, Fukumura D. Dissecting tumour pathophysiology using intravital microscopy. *Nat. Rev. Cancer.* 2002; 2:266–276. [PubMed: 12001988]
21. Correia AL, Bissell MJ. The tumor microenvironment is a dominant force in multidrug resistance. *Drug Resist. Updat.* 2012; 15:39–49. [PubMed: 22335920]
22. Trédan O, Galmarini CM, Patel K, Tannock IF. Drug resistance and the solid tumor microenvironment. *J. Natl Cancer Inst.* 2007; 99:1441–1454. [PubMed: 17895480]

23. Chauhan VP, Jain RK. Strategies for advancing cancer nanomedicine. *Nat. Mater.* 2013; 12:958–962. [PubMed: 24150413]
24. Wilhelm S, et al. Analysis of nanoparticle delivery to tumours. *Nat. Rev. Mater.* 2016; 1:16014.
25. Matsumura Y, Maeda HA. New concept for macromolecular therapeutics in cancer chemotherapy: mechanism of tumoritropic accumulation of proteins and the antitumor agent smancs. *Cancer Res.* 1986; 46:6387–6392. [PubMed: 2946403]
26. Gerlowski LE, Jain RK. Microvascular permeability of normal and neoplastic tissues. *Microvasc. Res.* 1986; 31:288–305. [PubMed: 2423854]
27. Dvorak HF, Brown LF, Detmar M, Dvorak AM. Vascular permeability factor/vascular endothelial growth factor, microvascular hyperpermeability, and angiogenesis. *Am. J. Pathol.* 1995; 146:1029–1039. [PubMed: 7538264]
28. Carmeliet P, Jain RK. Molecular mechanisms and clinical applications of angiogenesis. *Nature.* 2011; 473:298–307. [PubMed: 21593862]
29. Padera TP, et al. Cancer cells compress intratumour vessels. *Nature.* 2004; 427:695–695. [PubMed: 14973470]
30. Bertrand N, Wu J, Xu X, Kamaly N, Farokhzad OC. Cancer nanotechnology: the impact of passive and active targeting in the era of modern cancer biology. *Adv. Drug Deliv. Rev.* 2014; 66:2–25. [PubMed: 24270007]
31. Koukourakis MI, et al. Liposomal doxorubicin and conventionally fractionated radiotherapy in the treatment of locally advanced non-small-cell lung cancer and head and neck cancer. *J. Clin. Oncol.* 1999; 17:3512–3521. [PubMed: 10550149]
32. Stylianopoulos T, Jain RK. Design considerations for nanotherapeutics in oncology. *Nanomedicine.* 2015; 11:1893–1907. [PubMed: 26282377]
33. Jain RK, Baxter LT. Mechanisms of heterogeneous distribution of monoclonal antibodies and other macromolecules in tumors: significance of elevated interstitial pressure. *Cancer Res.* 1988; 48:7022–7032. Seminal paper on the role of elevated IFP as a barrier to drug delivery. [PubMed: 3191477]
34. Tong RT, et al. Vascular normalization by vascular endothelial growth factor receptor 2 blockade induces a pressure gradient across the vasculature and improves drug penetration in tumors. *Cancer Res.* 2004; 64:3731–3736. [PubMed: 15172975]
35. Batchelor TT, et al. Improved tumor oxygenation and survival in glioblastoma patients who show increased blood perfusion after cediranib and chemoradiation. *Proc. Natl Acad. Sci. USA.* 2013; 110:19059–19064. Clinical evidence that vascular normalization and the resulting increase in perfusion improve survival in cancer patients. [PubMed: 24190997]
36. Heist RS, et al. Improved tumor vascularization after anti-VEGF therapy with carboplatin and nab-paclitaxel associates with survival in lung cancer. *Proc. Natl Acad. Sci. USA.* 2015; 112:1547–1552. [PubMed: 25605928]
37. Tolaney SM, et al. Role of vascular density and normalization in response to neoadjuvant bevacizumab and chemotherapy in breast cancer patients. *Proc. Natl Acad. Sci. USA.* 2015; 112:14325–14330. [PubMed: 26578779]
38. US National Library of Medicine. 2017. [Clinicaltrials.govhttps://www.clinicaltrials.gov/ct2/show/NCT00662506](https://www.clinicaltrials.gov/ct2/show/NCT00662506)
39. US National Library of Medicine. 2017. [Clinicaltrials.govhttps://www.clinicaltrials.gov/ct2/show/NCT00642759](https://www.clinicaltrials.gov/ct2/show/NCT00642759)
40. Chauhan VP, et al. Angiotensin inhibition enhances drug delivery and potentiates chemotherapy by decompressing tumour blood vessels. *Nat. Commun.* 2013; 4:2516. [PubMed: 24084631]
41. Stylianopoulos T, et al. Causes, consequences, and remedies for growth-induced solid stress in murine and human tumors. *Proc. Natl Acad. Sci. USA.* 2012; 109:15101–15108. [PubMed: 22932871]
42. Nia HT, et al. Solid stress and elastic energy as measures of tumour mechanopathology. *Nat. Biomed. Eng.* 2016; 1:0004. [PubMed: 28966873]
43. Incio J, et al. Obesity-induced inflammation and desmoplasia promote pancreatic cancer progression and resistance to chemotherapy. *Cancer Discov.* 2016; 6:852–869. Study demonstrating the effects of obesity on tumour mechanics, along with potential strategies to

- overcome these effects using clinically available antifibrotic and inflammatory agents. [PubMed: 27246539]
44. Liu, H., et al. Use of angiotensin system inhibitors is associated with immune activation and longer survival in non-metastatic pancreatic ductal adenocarcinoma. *Clin. Cancer Res.* 2017. <http://dx.doi.org/10.1158/1078-0432.CCR-17-0256>
  45. Murphy JE, et al. TGF-B1 inhibition with losartan in combination with FOLFIRINOX (F-NOX) in locally advanced pancreatic cancer (LAPC): preliminary feasibility and R0 resection rates from a prospective phase II study. *J. Clin. Oncol.* 2017; 35:386–386.
  46. US National Library of Medicine. 2017. [Clinicaltrials.govhttps://clinicaltrials.gov/show/NCT01821729](https://clinicaltrials.gov/show/NCT01821729)
  47. Kalluri R. The biology and function of fibroblasts in cancer. *Nat. Rev. Cancer.* 2016; 16:582–598. [PubMed: 27550820]
  48. Provenzano PP, et al. Collagen density promotes mammary tumor initiation and progression. *BMC Med.* 2008; 6:11. [PubMed: 18442412]
  49. Levental KR, et al. Matrix crosslinking forces tumor progression by enhancing integrin signaling. *Cell.* 2009; 139:891–906. [PubMed: 19931152]
  50. Naba A, Clauser KR, Lamar JM, Carr SA, Hynes RO. Extracellular matrix signatures of human mammary carcinoma identify novel metastasis promoters. *eLife.* 2014; 3:e01308. [PubMed: 24618895]
  51. Provenzano PP, et al. Collagen reorganization at the tumor-stromal interface facilitates local invasion. *BMC Med.* 2006; 4:38. [PubMed: 17190588]
  52. Rivron NC, et al. Tissue deformation spatially modulates VEGF signaling and angiogenesis. *Proc. Natl Acad. Sci. USA.* 2012; 109:6886–6891. [PubMed: 22511716]
  53. Schrader J, et al. Matrix stiffness modulates proliferation, chemotherapeutic response, and dormancy in hepatocellular carcinoma cells. *Hepatology.* 2011; 53:1192–1205. [PubMed: 21442631]
  54. Youk JH, et al. Comparison of strain and shear wave elastography for the differentiation of benign from malignant breast lesions, combined with B-mode ultrasonography: qualitative and quantitative assessments. *Ultrasound Med. Biol.* 2014; 40:2336–2344. [PubMed: 25130444]
  55. Cheng G, Tse J, Jain RK, Munn LL. Microenvironmental mechanical stress controls tumor spheroid size and morphology by suppressing proliferation and inducing apoptosis in cancer cells. *PLoS ONE.* 2009; 4:e4632. [PubMed: 19247489]
  56. Calvo F, et al. Mechanotransduction and YAP-dependent matrix remodelling is required for the generation and maintenance of cancer-associated fibroblasts. *Nat. Cell Biol.* 2013; 15:637–646. [PubMed: 23708000]
  57. Paszek MJ, et al. Tensional homeostasis and the malignant phenotype. *Cancer Cell.* 2005; 8:241–254. Seminal work demonstrating that elevated tissue stiffness promotes malignant behaviour via modulation of integrins. [PubMed: 16169468]
  58. Wang K, et al. Stiffening and unfolding of early deposited-fibronectin increase proangiogenic factor secretion by breast cancer-associated stromal cells. *Biomaterials.* 2015; 54:63–71. [PubMed: 25907040]
  59. Artym VV, et al. Dense fibrillar collagen is a potent inducer of invadopodia via a specific signaling network. *J. Cell Biol.* 2015; 208:331–350. [PubMed: 25646088]
  60. Doyle AD, Carvajal N, Jin A, Matsumoto K, Yamada KM. Local 3D matrix microenvironment regulates cell migration through spatiotemporal dynamics of contractility-dependent adhesions. *Nat. Commun.* 2015; 6:8720. [PubMed: 26548801]
  61. Engler AJ, Sen S, Sweeney HL, Discher DE. Matrix elasticity directs stem cell lineage specification. *Cell.* 2006; 126:677–689. Seminal study demonstrating that stem cells that generate specialized cells within the body take cues from tissue stiffness to specify lineage and commit to phenotypes. [PubMed: 16923388]
  62. Bordeleau F, et al. Matrix stiffening promotes a tumor vasculature phenotype. *Proc. Natl Acad. Sci. USA.* 2017; 114:492–497. [PubMed: 28034921]
  63. Hynes RO. The extracellular matrix: not just pretty fibrils. *Science.* 2009; 326:1216–1219. [PubMed: 19965464]

64. Ulrich TA, De-Juan-Pardo EM, Kumar S. The mechanical rigidity of the extracellular matrix regulates the structure, motility, and proliferation of glioma cells. *Cancer Res.* 2009; 69:4167–4174. [PubMed: 19435897]
65. Weigelin B, Bakker G-J, Friedl P. Intravital third harmonic generation microscopy of collective melanoma cell invasion. *IntraVital.* 2012; 1:32–43.
66. Blehm BH, Jiang N, Kotobuki Y, Tanner K. Deconstructing the role of the ECM microenvironment on drug efficacy targeting MAPK signaling in a preclinical platform for cutaneous melanoma. *Biomaterials.* 2015; 56:129–139. [PubMed: 25934286]
67. Seo BR, et al. Obesity-dependent changes in interstitial ECM mechanics promote breast tumorigenesis. *Sci. Transl Med.* 2015; 7:301ra130. Study linking obesity, fibrotic remodelling and ECM mechanics to breast tumorigenesis.
68. Fukumura D, Incio J, Shankaraiah RC, Jain RK. Obesity and cancer: an angiogenic and inflammatory link. *Microcirculation.* 2016; 23:191–206. [PubMed: 26808917]
69. Laklai H, et al. Genotype tunes pancreatic ductal adenocarcinoma tissue tension to induce matricellular fibrosis and tumor progression. *Nat. Med.* 2016; 22:497–505. [PubMed: 27089513]
70. Bailey JM, et al. Sonic hedgehog promotes desmoplasia in pancreatic cancer. *Clin. Cancer Res.* 2008; 14:5995–6004. [PubMed: 18829478]
71. Olive KP, et al. Inhibition of hedgehog signaling enhances delivery of chemotherapy in a mouse model of pancreatic cancer. *Science.* 2009; 324:1457–1461. [PubMed: 19460966]
72. Rhim AD, et al. Stromal elements act to restrain, rather than support, pancreatic ductal adenocarcinoma. *Cancer Cell.* 2014; 25:735–747. [PubMed: 24856585]
73. Özdemir BC, et al. Depletion of carcinoma-associated fibroblasts and fibrosis induces immunosuppression and accelerates pancreas cancer with reduced survival. *Cancer Cell.* 2014; 25:719–734. [PubMed: 24856586]
74. Sherman MH, et al. Vitamin D receptor-mediated stromal reprogramming suppresses pancreatitis and enhances pancreatic cancer therapy. *Cell.* 2014; 159:80–93. [PubMed: 25259922]
75. Pinho SS, Reis CA. Glycosylation in cancer: mechanisms and clinical implications. *Nat. Rev. Cancer.* 2015; 15:540–555. [PubMed: 26289314]
76. Mitchell MJ, King MR. Physical Biology in Cancer. 3. The role of cell glycocalyx in vascular transport of circulating tumor cells. *Am. J. Physiol., Cell Physiol.* 2014; 306:C89–C97. [PubMed: 24133067]
77. Weinbaum S, Tarbell JM, Damiano ER. The structure and function of the endothelial glycocalyx layer. *Annu. Rev. Biomed. Eng.* 2007; 9:121–167. [PubMed: 17373886]
78. Hollingsworth MA, Swanson BJ. Mucins in cancer: protection and control of the cell surface. *Nat. Rev. Cancer.* 2004; 4:45–60. [PubMed: 14681689]
79. Itano N, Sawai T, Miyaishi O, Kimata K. Relationship between hyaluronan production and metastatic potential of mouse mammary carcinoma cells. *Cancer Res.* 1999; 59:2499–2504. [PubMed: 10344764]
80. Rahbari NN, et al. Anti-VEGF therapy induces ECM remodeling and mechanical barriers to therapy in colorectal cancer liver metastases. *Sci. Transl Med.* 2016; 8:360ra135.
81. Paszek MJ, et al. The cancer glycocalyx mechanically primes integrin-mediated growth and survival. *Nature.* 2014; 511:319–325. First study implicating the bulky glycocalyx of tumour cells as a feature that promotes metastasis via mechanically enhanced cell-surface-receptor function. [PubMed: 25030168]
82. Hudak JE, Canham SM, Bertozzi CR. Glycocalyx engineering reveals a Siglec-based mechanism for NK cell immunoevasion. *Nature Chem. Biol.* 2013; 10:69–75. [PubMed: 24292068]
83. Läubli H, et al. Engagement of myelomonocytic Siglecs by tumor-associated ligands modulates the innate immune response to cancer. *Proc. Natl Acad. Sci. USA.* 2014; 111:14211–14216. [PubMed: 25225409]
84. Xiao H, Woods EC, Vukojicic P, Bertozzi CR. Precision glycocalyx editing as a strategy for cancer immunotherapy. *Proc. Natl Acad. Sci. USA.* 2016; 113:10304–10309. [PubMed: 27551071]
85. Langer R, Folkman J. Polymers for the sustained release of proteins and other macromolecules. *Nature.* 1976; 263:797–800. First demonstration of the use of polymeric materials for controlled, sustained release of high-molecular-weight compounds for > 100 days. [PubMed: 995197]

86. Yatvin MB, Weinstein JN, Dennis WH, Blumenthal R. Design of liposomes for enhanced local release of drugs by hyperthermia. *Science*. 1978; 202:1290–1293. [PubMed: 364652]
87. Brownlee M, Cerami A. A glucose-controlled insulin-delivery system: semisynthetic insulin bound to lectin. *Science*. 1979; 206:1190–1191. [PubMed: 505005]
88. Steichen SD, Caldorera-Moore M, Peppas NA. A review of current nanoparticle and targeting moieties for the delivery of cancer therapeutics. *Eur. J. Pharm. Sci.* 2013; 48:416–427. [PubMed: 23262059]
89. Langer R. Drug delivery and targeting. *Nature*. 1998; 392:5–10. [PubMed: 9579855]
90. Sampath P, Brem H. Implantable slow-release chemotherapeutic polymers for the treatment of malignant brain tumors. *Cancer Control*. 1998; 5:130–137. [PubMed: 10761024]
91. Okada H, Doken Y, Ogawa Y, Toguchi H. Preparation of three-month depot injectable microspheres of leuprorelin acetate using biodegradable polymers. *Pharm. Res.* 1994; 11:1143–1147. [PubMed: 7971715]
92. Gabizon A, et al. Prolonged circulation time and enhanced accumulation in malignant exudates of doxorubicin encapsulated in polyethylene-glycol coated liposomes. *Cancer Res.* 1994; 54:987–992. Seminal report showing prolonged circulation time and enhanced tumour accumulation of polyethylene glycol-coated doxorubicin liposome formulations (Doxil) in patients, compared with free doxorubicin. [PubMed: 8313389]
93. Gu L, Mooney DJ. Biomaterials and emerging anticancer therapeutics: engineering the microenvironment. *Nat. Rev. Cancer*. 2016; 16:56–66. [PubMed: 26694936]
94. Moon JJ, Huang B, Irvine DJ. Engineering nano- and microparticles to tune immunity. *Adv. Mater.* 2012; 24:3724–3746. [PubMed: 22641380]
95. Liu H, et al. Structure-based programming of lymph-node targeting in molecular vaccines. *Nature*. 2014; 507:519–522. Engineering of an amphiphilic cancer vaccine that ‘hitchhikes’ with serum albumin to traffic efficiently to lymph nodes, enabling substantially increased potency and safety of subunit vaccines. [PubMed: 24531764]
96. Jeanbart L, et al. Enhancing efficacy of anticancer vaccines by targeted delivery to tumor-draining lymph nodes. *Cancer Immunol. Res.* 2014; 2:436–447. [PubMed: 24795356]
97. Thomas SN, Vokali E, Lund AW, Hubbell JA, Swartz MA. Targeting the tumor-draining lymph node with adjuvanted nanoparticles reshapes the antitumor immune response. *Biomaterials*. 2014; 35:814–824. [PubMed: 24144906]
98. Kranz LM, et al. Systemic RNA delivery to dendritic cells exploits antiviral defence for cancer immunotherapy. *Nature*. 2016; 534:396–401. Synthesis of a nanoparticle RNA vaccine that targets dendritic cells after systemic administration, leading to an antitumour immune response with antiviral features as well as potential efficacy in patients with advanced melanoma. [PubMed: 27281205]
99. US National Library of Medicine. 2016. [Clinicaltrials.govhttps://clinicaltrials.gov/ct2/show/NCT02410733](https://clinicaltrials.gov/ct2/show/NCT02410733)
100. Chahal JS, et al. Dendrimer-RNA nanoparticles generate protective immunity against lethal Ebola, H1N1 influenza, and *Toxoplasma gondii* challenges with a single dose. *Proc. Natl Acad. Sci. USA*. 2016; 113:E4133–E4142. [PubMed: 27382155]
101. Restifo NP, Dudley ME, Rosenberg SA. Adoptive immunotherapy for cancer: harnessing the T cell response. *Nat. Rev. Immunol.* 2012; 12:269–281. [PubMed: 22437939]
102. Stephan MT, Moon JJ, Um SH, Bershteyn A, Irvine DJ. Therapeutic cell engineering with surface-conjugated synthetic nanoparticles. *Nat. Med.* 2010; 16:1035–1041. [PubMed: 20711198]
103. Stephan MT, Stephan SB, Bak P, Chen J, Irvine DJ. Synapse-directed delivery of immunomodulators using T-cell-conjugated nanoparticles. *Biomaterials*. 2012; 33:5776–5787. [PubMed: 22594972]
104. Huang B, et al. Active targeting of chemotherapy to disseminated tumors using nanoparticle-carrying T cells. *Sci. Transl Med.* 2015; 7:291ra94.
105. Mitchell MJ, Wayne E, Rana K, Schaffer CB, King MR. TRAIL-coated leukocytes that kill cancer cells in the circulation. *Proc. Natl Acad. Sci. USA*. 2014; 111:930–935. [PubMed: 24395803]

106. Mitchell MJ, King MR. Leukocytes as carriers for targeted cancer drug delivery. *Expert Opin. Drug Deliv.* 2014; 12:375–392. [PubMed: 25270379]
107. Mitchell MJ, et al. Polymeric mechanical amplifiers of immune cytokine-mediated apoptosis. *Nat. Commun.* 2017; 8:14179. [PubMed: 28317839]
108. Wayne EC, et al. TRAIL-coated leukocytes that prevent the bloodborne metastasis of prostate cancer. *J. Control. Release.* 2016; 223:215–223. [PubMed: 26732555]
109. Zuckerman JE, Davis ME. Clinical experiences with systemically administered siRNA-based therapeutics in cancer. *Nat. Rev. Drug Discov.* 2015; 14:843–856. [PubMed: 26567702]
110. US National Library of Medicine. 2017. [ClinicalTrials.gov](https://clinicaltrials.gov/ct2/show/NCT01960348) <https://clinicaltrials.gov/ct2/show/NCT01960348>
111. Davis ME, et al. Evidence of RNAi in humans from systemically administered siRNA via targeted nanoparticles. *Nature.* 2010; 464:1067–1070. [PubMed: 20305636]
112. US National Library of Medicine. 2013. [ClinicalTrials.gov](https://clinicaltrials.gov/ct2/show/NCT00938574) <https://clinicaltrials.gov/ct2/show/NCT00938574>
113. US National Library of Medicine. 2017. [ClinicalTrials.gov](https://clinicaltrials.gov/ct2/show/NCT01591356) <https://clinicaltrials.gov/ct2/show/NCT01591356>
114. Yin H, et al. Non-viral vectors for gene-based therapy. *Nat. Rev. Genet.* 2014; 15:541–555. [PubMed: 25022906]
115. Zhu X, et al. Long-circulating siRNA nanoparticles for validating Prohibitin1-targeted non-small cell lung cancer treatment. *Proc. Natl Acad. Sci. USA.* 2015; 112:7779–7784. [PubMed: 26056316]
116. Ren Y, et al. Targeted tumor-penetrating siRNA nanocomplexes for credentialing the ovarian cancer oncogene ID4. *Sci. Transl Med.* 2012; 4:147ra112.
117. Jensen SA, et al. Spherical nucleic acid nanoparticle conjugates as an RNAi-based therapy for glioblastoma. *Sci. Transl Med.* 2013; 5:209ra152.
118. Dahlman JE, et al. *In vivo* endothelial siRNA delivery using polymeric nanoparticles with low molecular weight. *Nat. Nanotechnol.* 2014; 9:648–655. [PubMed: 24813696]
119. Akinc A, et al. Targeted delivery of RNAi therapeutics with endogenous and exogenous ligand-based mechanisms. *Mol. Ther.* 2010; 18:1357–1364. [PubMed: 20461061]
120. Xue W, et al. Small RNA combination therapy for lung cancer. *Proc. Natl Acad. Sci. USA.* 2014; 111:E3553–E3561. [PubMed: 25114235]
121. Deng ZJ, et al. Layer-by-layer nanoparticles for systemic codelivery of an anticancer drug and siRNA for potential triple-negative breast cancer treatment. *ACS Nano.* 2013; 7:9571–9584. [PubMed: 24144228]
122. Zhao Y, et al. PolyMetformin combines carrier and anticancer activities for *in vivo* siRNA delivery. *Nat. Commun.* 2016; 7:11822. [PubMed: 27264609]
123. Coombes RC. Drug testing in the patient: toward personalized cancer treatment. *Sci. Transl Med.* 2015; 7:284ps10.
124. Jonas O, et al. An implantable microdevice to perform high-throughput *in vivo* drug sensitivity testing in tumors. *Sci. Transl Med.* 2015; 7:284ra57. Development of a minimally invasive microdevice that can be implanted and removed from tumours using a biopsy needle, enabling direct drug sensitivity testing of many compounds within a patient.
125. Klinghoffer RA, et al. A technology platform to assess multiple cancer agents simultaneously within a patient's tumor. *Sci. Transl Med.* 2015; 7:284ra58.
126. US National Library of Medicine. 2017. [ClinicalTrials.gov](https://clinicaltrials.gov/ct2/show/NCT01831505) <https://clinicaltrials.gov/ct2/show/NCT01831505>
127. US National Library of Medicine. 2017. [ClinicalTrials.gov](https://clinicaltrials.gov/ct2/show/NCT03056599) <https://clinicaltrials.gov/ct2/show/NCT03056599>
128. Yin H, Kauffman KJ, Anderson DG. Delivery technologies for genome editing. *Nat. Rev. Drug Discov.* 2017; 16:387–399. [PubMed: 28337020]
129. Weissleder R, Nahrendorf M. Advancing biomedical imaging. *Proc. Natl Acad. Sci. USA.* 2015; 112:14424–14428. [PubMed: 26598657]



130. Bao G, Mitragotri S, Tong S. Multifunctional nanoparticles for drug delivery and molecular imaging. *Annu. Rev. Biomed. Eng.* 2013; 15:253–282. [PubMed: 23642243]
131. Rimm DL. What brown cannot do for you. *Nat. Biotechnol.* 2006; 24:914–916. [PubMed: 16900128]
132. Angelo M, et al. Multiplexed ion beam imaging of human breast tumors. *Nat. Med.* 2014; 20:436–442. Development of a new technique — multiplex ion beam imaging — which utilizes secondary ion mass spectrometry and antibodies labelled with isotopically pure elemental metals to detect up to 100 tumour antigens within a single sample. [PubMed: 24584119]
133. Bendall SC, et al. Single-cell mass cytometry of differential immune and drug responses across a human hematopoietic continuum. *Science.* 2011; 332:687–696. [PubMed: 21551058]
134. Peet AC, Arvanitis TN, Leach MO, Waldman AD. Functional imaging in adult and paediatric brain tumours. *Nat. Rev. Clin. Oncol.* 2012; 9:700–711. [PubMed: 23149894]
135. Choi C, et al. 2-Hydroxyglutarate detection by magnetic resonance spectroscopy in IDH-mutated patients with gliomas. *Nat. Med.* 2012; 18:624–629. [PubMed: 22281806]
136. Zackrisson S, van de Ven SMWY, Gambhir SS. Light in and sound out: emerging translational strategies for photoacoustic imaging. *Cancer Res.* 2014; 74:979–1004. [PubMed: 24514041]
137. Jokerst JV, Cole AJ, Van de Sompel D, Gambhir SS. Gold nanorods for ovarian cancer detection with photoacoustic imaging and resection guidance via Raman imaging in living mice. *ACS Nano.* 2012; 6:10366–10377. [PubMed: 23101432]
138. la Zerda, de A., et al. Family of enhanced photoacoustic imaging agents for high-sensitivity and multiplexing studies in living mice. *ACS Nano.* 2012; 6:4694–4701. [PubMed: 22607191]
139. Kircher MF, et al. A brain tumor molecular imaging strategy using a new triple-modality MRI-photoacoustic-Raman nanoparticle. *Nat. Med.* 2012; 18:829–834. [PubMed: 22504484]
140. Pu K, et al. Semiconducting polymer nanoparticles as photoacoustic molecular imaging probes in living mice. *Nat. Nanotechnol.* 2014; 9:233–239. [PubMed: 24463363]
141. Jokerst JV, Lobovkina T, Zare RN, Gambhir SS. Nanoparticle PEGylation for imaging and therapy. *Nanomedicine.* 2011; 6:715–728. [PubMed: 21718180]
142. Gu F, et al. Precise engineering of targeted nanoparticles by using self-assembled biointegrated block copolymers. *Proc. Natl Acad. Sci. USA.* 2008; 105:2586–2591. [PubMed: 18272481]
143. Ruoslahti E, Bhatia SN, Sailor MJ. Targeting of drugs and nanoparticles to tumors. *J. Cell Biol.* 2010; 188:759–768. [PubMed: 20231381]
144. Ghosh D, et al. M13-templated magnetic nanoparticles for targeted *in vivo* imaging of prostate cancer. *Nat. Nanotechnology.* 2012; 7:677–682.
145. Weissleder R, Schwaiger MC, Gambhir SS, Hricak H. Imaging approaches to optimize molecular therapies. *Sci. Transl Med.* 2016; 8:355ps16.
146. Miller MA, Weissleder R. Imaging the pharmacology of nanomaterials by intravital microscopy: toward understanding their biological behavior. *Adv. Drug Deliv. Rev.* 2016; 113:61–86. [PubMed: 27266447]
147. Thurber GM, et al. Single-cell and subcellular pharmacokinetic imaging allows insight into drug action *in vivo*. *Nat. Commun.* 2013; 4:1504. [PubMed: 23422672]
148. Laughney AM, et al. Single-cell pharmacokinetic imaging reveals a therapeutic strategy to overcome drug resistance to the microtubule inhibitor eribulin. *Sci. Transl Med.* 2014; 6:261ra152.
149. Miller MA, Askevold B, Yang KS, Kohler RH, Weissleder R. Platinum compounds for high-resolution *in vivo* cancer imaging. *ChemMedChem.* 2014; 9:1131–1135. [PubMed: 24504646]
150. Dubach JM, et al. *In vivo* imaging of specific drug-target binding at subcellular resolution. *Nat. Commun.* 2014; 5:3946. [PubMed: 24867710]
151. Miller MA, et al. Tumour-associated macrophages act as a slow-release reservoir of nano-therapeutic Pt(IV) pro-drug. *Nat. Commun.* 2015; 6:8692. [PubMed: 26503691]
152. Miller MA, et al. Predicting therapeutic nanomedicine efficacy using a companion magnetic resonance imaging nanoparticle. *Sci. Transl Med.* 2015; 7:314ra183. A combined approach of MRI and intravital imaging, which demonstrated that magnetic nanoparticles can be used to

select for tumours *in vivo* with high EPR and thus are more likely to respond to treatment with therapeutic nanoparticles.

153. Harisinghani MG, et al. A pilot study of lymphotropic nanoparticle-enhanced magnetic resonance imaging technique in early stage testicular cancer: a new method for noninvasive lymph node evaluation. *Urology*. 2005; 66:1066–1071. [PubMed: 16286125]
154. Wyckoff J, Gligorijevic B, Entenberg D, Segall J, Condeelis J. High-resolution multiphoton imaging of tumors *in vivo*. *Cold Spring Harb. Protoc.* 2011; 2011:1167–1184. [PubMed: 21969629]
155. Jain RK. Normalizing tumor vasculature with antiangiogenic therapy: a new paradigm for combination therapy. *Nat. Med.* 2001; 7:987–989. Seminal paper to put forward the vascular normalization hypothesis that changed the paradigm in antiangiogenic therapy. [PubMed: 11533692]
156. Wang W, et al. Coordinated regulation of pathways for enhanced cell motility and chemotaxis is conserved in rat and mouse mammary tumors. *Cancer Res.* 2007; 67:3505–3511. [PubMed: 17440055]
157. Wyckoff J, et al. A paracrine loop between tumor cells and macrophages is required for tumor cell migration in mammary tumors. *Cancer Res.* 2004; 64:7022–7029. [PubMed: 15466195]
158. Lohela M, et al. Intravital imaging reveals distinct responses of depleting dynamic tumor-associated macrophage and dendritic cell subpopulations. *Proc. Natl Acad. Sci. USA.* 2014; 111:E5086–E5095. [PubMed: 25385645]
159. Goswami S, et al. Macrophages promote the invasion of breast carcinoma cells via a colony-stimulating factor-1/epidermal growth factor paracrine loop. *Cancer Res.* 2005; 65:5278–5283. [PubMed: 15958574]
160. Wyckoff JB, et al. Direct visualization of macrophage-assisted tumor cell intravasation in mammary tumors. *Cancer Res.* 2007; 67:2649–2656. [PubMed: 17363585]
161. Peterson TE, et al. Dual inhibition of Ang-2 and VEGF receptors normalizes tumor vasculature and prolongs survival in glioblastoma by altering macrophages. *Proc. Natl Acad. Sci. USA.* 2016; 113:4470–4475. [PubMed: 27044097]
162. Brown E, et al. Dynamic imaging of collagen and its modulation in tumors *in vivo* using second-harmonic generation. *Nat. Med.* 2003; 9:796–800. [PubMed: 12754503]
163. Nadiarnykh O, LaComb RB, Brewer MA, Campagnola PJ. Alterations of the extracellular matrix in ovarian cancer studied by Second Harmonic Generation imaging microscopy. *BMC Cancer.* 2010; 10:94. [PubMed: 20222963]
164. Conklin MW, et al. Aligned collagen is a prognostic signature for survival in human breast carcinoma. *Am. J. Pathol.* 2011; 178:1221–1232. [PubMed: 21356373]
165. Gailhouste L, et al. Fibrillar collagen scoring by second harmonic microscopy: a new tool in the assessment of liver fibrosis. *J. Hepatol.* 2010; 52:398–406. [PubMed: 20149472]
166. Weigelin B, Bakker G-J, Friedl P. Third harmonic generation microscopy of cells and tissue organization. *J. Cell Sci.* 2016; 129:245–255. [PubMed: 26743082]
167. Lambert AW, Pattabiraman DR, Weinberg RA. Emerging biological principles of metastasis. *Cell.* 2017; 168:670–691. [PubMed: 28187288]
168. Bruns OT, et al. Next-generation *in vivo* optical imaging with short-wave infrared quantum dots. *Nat. Biomed. Eng.* 2017; 1:0056. [PubMed: 29119058]
169. Errico C, et al. Ultrafast ultrasound localization microscopy for deep super-resolution vascular imaging. *Nature.* 2015; 527:499–502. [PubMed: 26607546]
170. Nelson SJ, et al. Metabolic imaging of patients with prostate cancer using hyperpolarized [1-<sup>13</sup>C]pyruvate. *Sci. Transl Med.* 2013; 5:198ra108.
171. Walker-Samuel S, et al. *In vivo* imaging of glucose uptake and metabolism in tumors. *Nat. Med.* 2013; 19:1067–1072. [PubMed: 23832090]
172. Shields JD, et al. Autologous chemotaxis as a mechanism of tumor cell homing to lymphatics via interstitial flow and autocrine CCR7 signaling. *Cancer Cell.* 2007; 11:526–538. Seminal study identifying a novel mechanism underlying metastasis through the lymphatic system, named autologous chemotaxis, which directs tumour cell migration via autocrine chemokine gradients induced by interstitial flow. [PubMed: 17560334]

173. Polacheck WJ, Charest JL, Kamm RD. Interstitial flow influences direction of tumor cell migration through competing mechanisms. *Proc. Natl Acad. Sci. USA.* 2011; 108:11115–11120. [PubMed: 21690404]
174. Paul CD, Mistriotis P, Konstantopoulos K. Cancer cell motility: lessons from migration in confined spaces. *Nat. Rev. Cancer.* 2016; 17:131–140. [PubMed: 27909339]
175. Mekhdjian AH, et al. Integrin-mediated traction force enhances paxillin molecular associations and adhesion dynamics that increase the invasiveness of tumor cells into a three-dimensional extracellular matrix. *Mol. Biol. Cell.* 2017; 28:1467–1488. [PubMed: 28381423]
176. Alexander S, Weigelin B, Winkler F, Friedl P. Preclinical intravital microscopy of the tumour-stroma interface: invasion, metastasis, and therapy response. *Curr. Opin. Cell Biol.* 2013; 25:659–671. [PubMed: 23896198]
177. Kraning-Rush CM, Carey SP, Lampi MC. Microfabricated collagen tracks facilitate single cell metastatic invasion in 3D. *Integr. Biol.* 2013; 5:606–616.
178. Carey SP, et al. Comparative mechanisms of cancer cell migration through 3D matrix and physiological microtracks. *Am. J. Physiol., Cell Physiol.* 2015; 308:C436–C447. [PubMed: 25500742]
179. Pathak A, Kumar S. Independent regulation of tumor cell migration by matrix stiffness and confinement. *Proc. Natl Acad. Sci.* 2012; 109:10334–10339. [PubMed: 22689955]
180. Stroka KM, et al. Water permeation drives tumor cell migration in confined microenvironments. *Cell.* 2014; 157:611–623. [PubMed: 24726433]
181. Raab M, et al. ESCRT III repairs nuclear envelope ruptures during cell migration to limit DNA damage and cell death. *Science.* 2016; 352:359–362. [PubMed: 27013426]
182. Denais CM, et al. Nuclear envelope rupture and repair during cancer cell migration. *Science.* 2016; 352:353–358. [PubMed: 27013428]
183. Irianto J, et al. DNA damage follows repair factor depletion and portends genome variation in cancer cells after pore migration. *Curr. Biol.* 2017; 27:210–223. [PubMed: 27989676]
184. Irianto J, et al. Nuclear constriction segregates mobile nuclear proteins away from chromatin. *Mol. Biol. Cell.* 2016; 27:4011–4020. [PubMed: 27798234]
185. Esch EW, Bahinski A, Huh D. Organs-on-chips at the frontiers of drug discovery. *Nat. Rev. Drug Discov.* 2015; 14:248–260. [PubMed: 25792263]
186. Song JW, et al. Microfluidic endothelium for studying the intravascular adhesion of metastatic breast cancer cells. *PLoS ONE.* 2009; 4:e5756. [PubMed: 19484126]
187. Bersini S, et al. A microfluidic 3D *in vitro* model for specificity of breast cancer metastasis to bone. *Biomaterials.* 2013; 35:2454–2461. [PubMed: 24388382]
188. Sung JH, Shuler ML. A micro cell culture analog ( $\mu$ CCA) with 3D hydrogel culture of multiple cell lines to assess metabolism-dependent cytotoxicity of anti-cancer drugs. *Lab Chip.* 2009; 9:1385–1394. Early work using organs-on-chip models, demonstrating that microfluidic devices combined with 3D hydrogel cell cultures representing individual organs can accurately reproduce anticancer drug effects observed *in vivo*. [PubMed: 19417905]
189. Sung JH, Kam C, Shuler ML. A microfluidic device for a pharmacokinetic-pharmacodynamic (PK-PD) model on a chip. *Lab Chip.* 2010; 10:446–455. [PubMed: 20126684]
190. Yu M, Stott S, Toner M, Maheswaran S, Haber DA. Circulating tumor cells: approaches to isolation and characterization. *J. Cell Biol.* 2011; 192:373–382. [PubMed: 21300848]
191. Yu M, et al. *Ex vivo* culture of circulating breast tumor cells for individualized testing of drug susceptibility. *Science.* 2014; 345:216–220. [PubMed: 25013076]
192. Murlidhar V, Rivera-Báez L, Nagrath S. Affinity versus label-free isolation of circulating tumor cells: who wins? *Small.* 2016; 12:4450–4463. [PubMed: 27436104]
193. Nagrath S, et al. Isolation of rare circulating tumour cells in cancer patients by microchip technology. *Nature.* 2007; 450:1235–1239. Seminal study that developed a unique flow-based microfluidic platform containing antibody-coated microposts to isolate rare CTCs from the blood of patients with metastatic cancer. [PubMed: 18097410]
194. Yoon HJ, et al. Sensitive capture of circulating tumour cells by functionalized graphene oxide nanosheets. *Nat. Nanotechnol.* 2013; 8:735–741. [PubMed: 24077027]

195. Gleghorn JP, et al. Capture of circulating tumor cells from whole blood of prostate cancer patients using geometrically enhanced differential immunocapture (GEDI) and a prostate-specific antibody. *Lab Chip*. 2010; 10:27–29. [PubMed: 20024046]
196. Ozkumur E, et al. Inertial focusing for tumor antigen-dependent and -independent sorting of rare circulating tumor cells. *Sci. Transl Med*. 2013; 5:179ra47.
197. Hou J-M, et al. Clinical significance and molecular characteristics of circulating tumor cells and circulating tumor microemboli in patients with small cell lung cancer. *J. Clin. Oncol*. 2012; 30:525–532. [PubMed: 22253462]
198. Cheung KJ, Ewald AJ. A collective route to metastasis: seeding by tumor cell clusters. *Science*. 2016; 352:167–169. [PubMed: 27124449]
199. Cheung KJ, et al. Polyclonal breast cancer metastases arise from collective dissemination of keratin 14-expressing tumor cell clusters. *Proc. Natl Acad. Sci. USA*. 2016; 113:E854–E863. [PubMed: 26831077]
200. Sarioglu AF, et al. A microfluidic device for label-free, physical capture of circulating tumor cell clusters. *Nat. Methods*. 2015; 12:685–691. [PubMed: 25984697]
201. Hoshino A, et al. Tumour exosome integrins determine organotropic metastasis. *Nature*. 2015; 527:329–335. [PubMed: 26524530]
202. Liga A, Vliegenthart A, Oosthuizen W, Dear JW, Kersaudy-Kerhoas M. Exosome isolation: a microfluidic road-map. *Lab Chip*. 2015; 15:2388–2394. [PubMed: 25940789]
203. Chen C, et al. Microfluidic isolation and transcriptome analysis of serum microvesicles. *Lab Chip*. 2010; 10:505–511. [PubMed: 20126692]
204. Im H, et al. Label-free detection and molecular profiling of exosomes with a nano-plasmonic sensor. *Nat. Biotechnol*. 2014; 32:490–495. [PubMed: 24752081]
205. Wunsch BH, et al. Nanoscale lateral displacement arrays for the separation of exosomes and colloids down to 20 nm. *Nat. Nanotechnol*. 2016; 11:936–940. [PubMed: 27479757]
206. Farrell D, et al. Recent advances from the National Cancer Institute Alliance for Nanotechnology in Cancer. *ACS Nano*. 2010; 4:589–594. [PubMed: 20175564]
207. Kuhn NZ, Nagahara LA. Integrating physical sciences perspectives in cancer research. *Sci. Transl Med*. 2013; 5:183fs14.
208. Sharp P, Hockfield S. Convergence: the future of health. *Science*. 2017; 355:589–589.
209. Ewald AJ, Egeblad M. Cancer: sugar-coated cell signalling. *Nature*. 2014; 511:298–299. [PubMed: 25030162]
210. De Vries J, Figdor C. Immunotherapy: cancer vaccine triggers antiviral-type defences. *Nature*. 2016; 534:329–331. [PubMed: 27281206]
211. Speicher MR, Pantel K. Tumor signatures in the blood. *Nat. Biotechnol*. 2014; 32:441–443. [PubMed: 24811515]

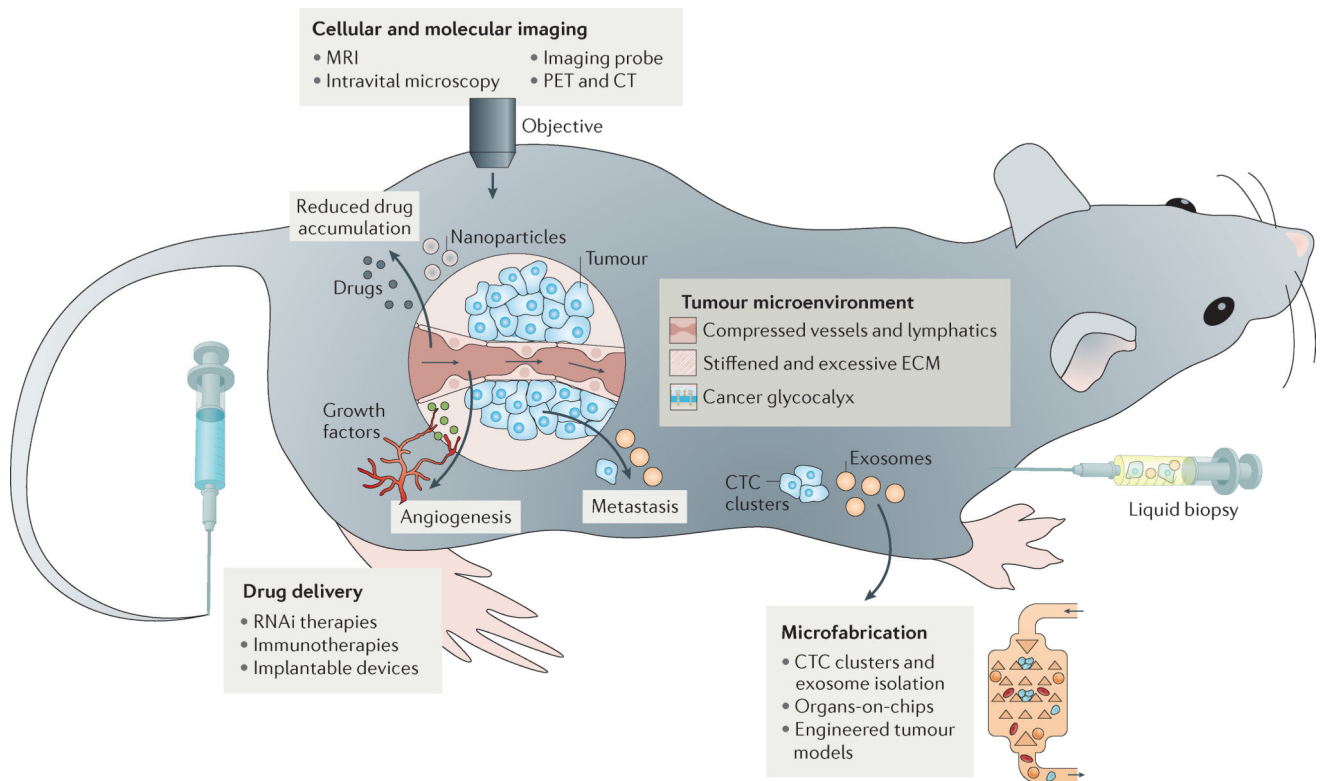


**Figure 1. An overview of engineering and physical sciences in oncology**

Physical abnormalities of the tumour microenvironment (TME) have been identified using tools and concepts from engineering and the physical sciences. These include blood vessel and lymphatic compression, stiffened and excessive extracellular matrix (ECM), and the cancer cell glycolyx. Collapsed blood vessels and increased solid stresses lead to reduced accumulation and limited delivery of drugs to tumour tissues. Steep pressure gradients in the periphery push fluid leaking from blood vessels located in the tumour margin into the surrounding normal tissues, facilitating the transport of growth factors and cancer cells into normal tissue and thus fuelling tumour growth, angiogenesis and metastasis. Pressure gradients also reduce the retention time of drugs and inhibit their homogeneous distribution inside the tumour. Advances in imaging, drug delivery and microfabrication have all been used to detect, manipulate and therapeutically target various aspects of this microenvironment. CT, computed tomography; CTC, circulating tumour cell; MRI, magnetic resonance imaging; PET, positron emission tomography.

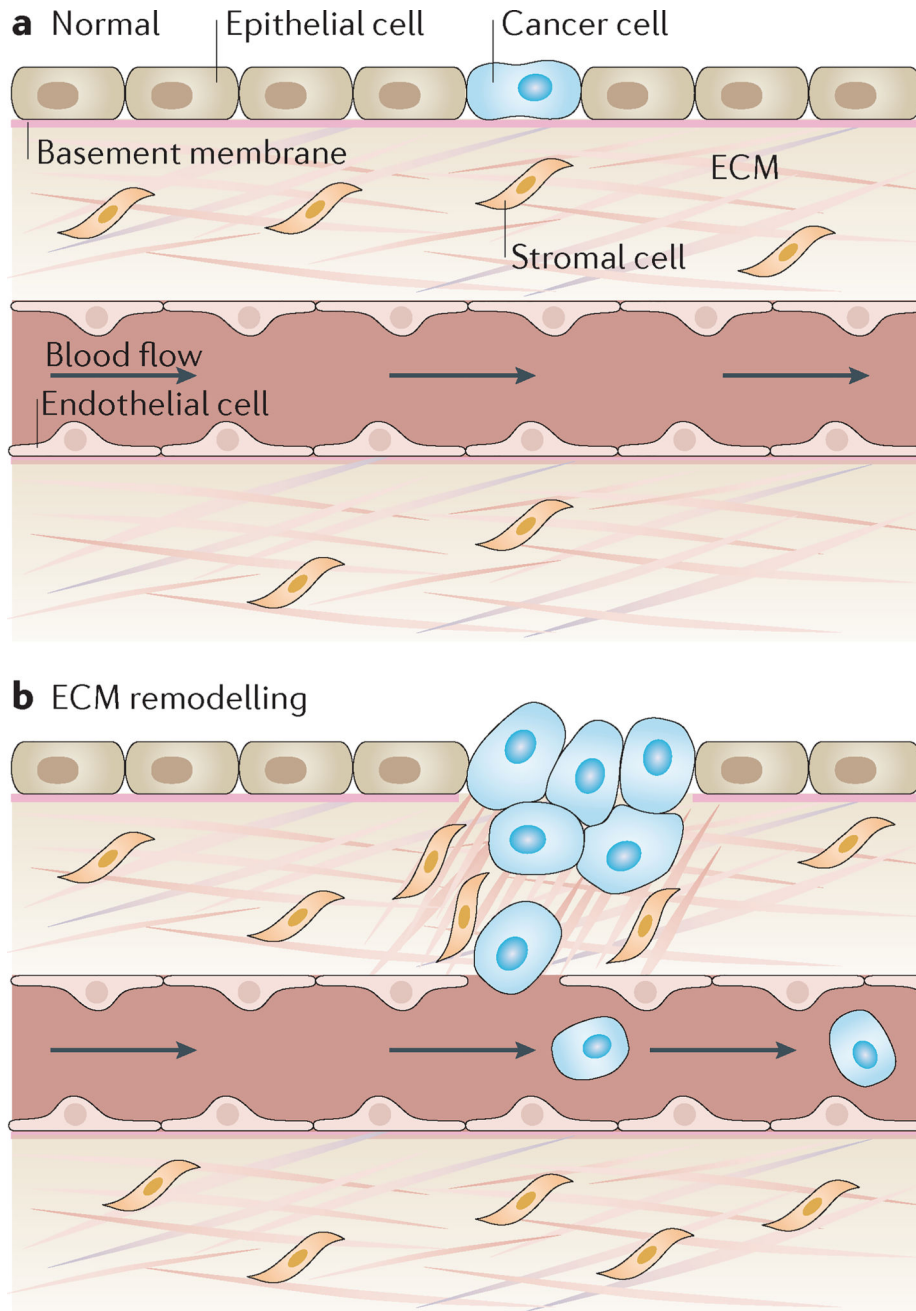


**Figure 2. Extracellular matrix stiffening promotes cancer progression**

**a** | Under homeostatic conditions, the extracellular matrix (ECM) maintains tissue integrity and blocks rare tumour-prone cells from malignant progression by maintaining an overall healthy microenvironment. **b** | Under pathological conditions, ECM remodelling leads to collagen fibre alignment, bundling, and stiffening, which in turn alter interactions between the matrix and stromal and tumour cells to enhance pro-angiogenic secretion from a range of cells in the microenvironment as well as the migration of cancer cells. This process consequently promotes both the invasion of tumour cells from the primary site into the

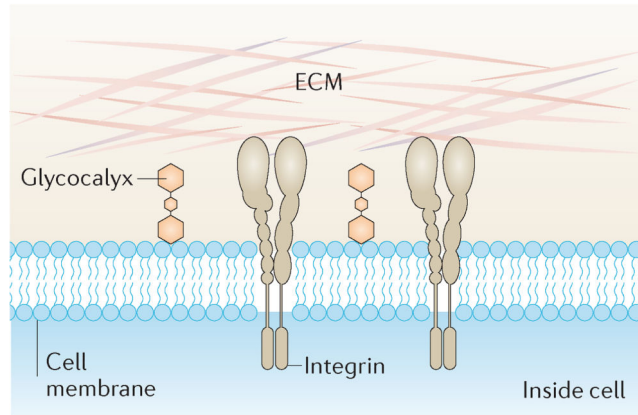
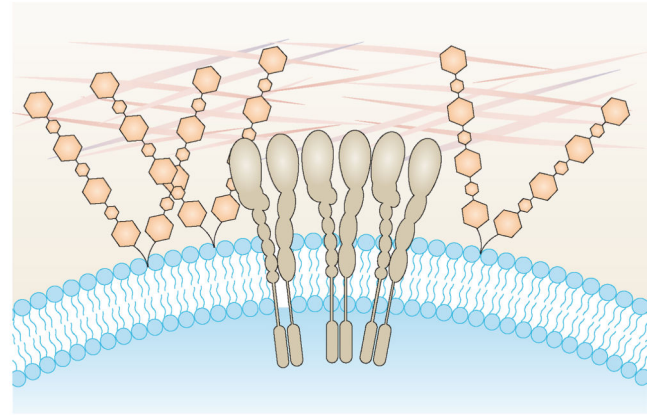
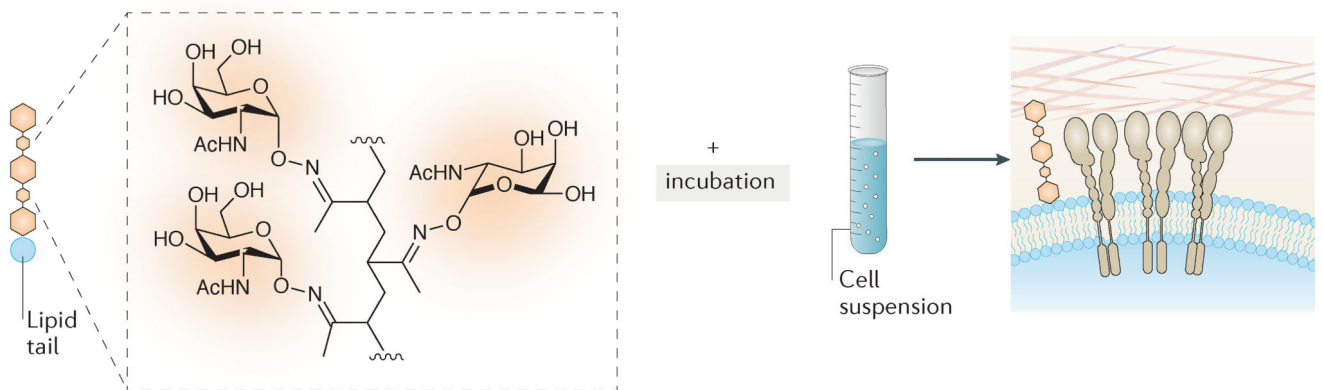
circulation and the recruitment of endothelial cells for vascularization of the tumour to initiate tumour growth, invasion into the surrounding stroma and, finally, metastasis<sup>3</sup>.

Author Manuscript

Author Manuscript

Author Manuscript

Author Manuscript

**a** Normal glycoalyx**b** Large glycoalyx**c** Glycoprotein mimetic**Figure 3. Role of the cancer cell glycoalyx in cancer progression**

**a** | Normal cells with a short glycoalyx have a uniform distribution of glycoproteins and adhesion molecules (integrins) across the cell membrane, which is close to the surrounding extracellular matrix (ECM). **b** | Cells with a larger glycoalyx, such as tumour cells<sup>81</sup>, exhibit extended gaps between the membrane and ECM, clustering of integrins, the exclusion of glycopolymers from regions of integrin adhesion, and membrane bending. These physical effects can alter cell signalling and promote tumour survival. **c** | Engineering the cancer cell glycoalyx via incorporation of synthetic glycoprotein mimetics with lipid insertion domains into living cell membranes<sup>81</sup>. The glycopolymers consist of a long-chain polymer backbone, pendant glycan chains mimicking natural mucin *O*-glycans, a phospholipid insertion domain and a fluorophore for imaging incorporation into cells. The approach enables synthetic mucin glycoprotein mimetics of a range of lengths to be rapidly incorporated into plasma membranes, where they project perpendicular to the cell surface. Synthetic glycoprotein mimetics have been used to study how the physical properties of the glycoalyx coating regulate cell survival during tumour invasion. Parts **a** and **b** are from REF. 209, Macmillan Publishers Limited.



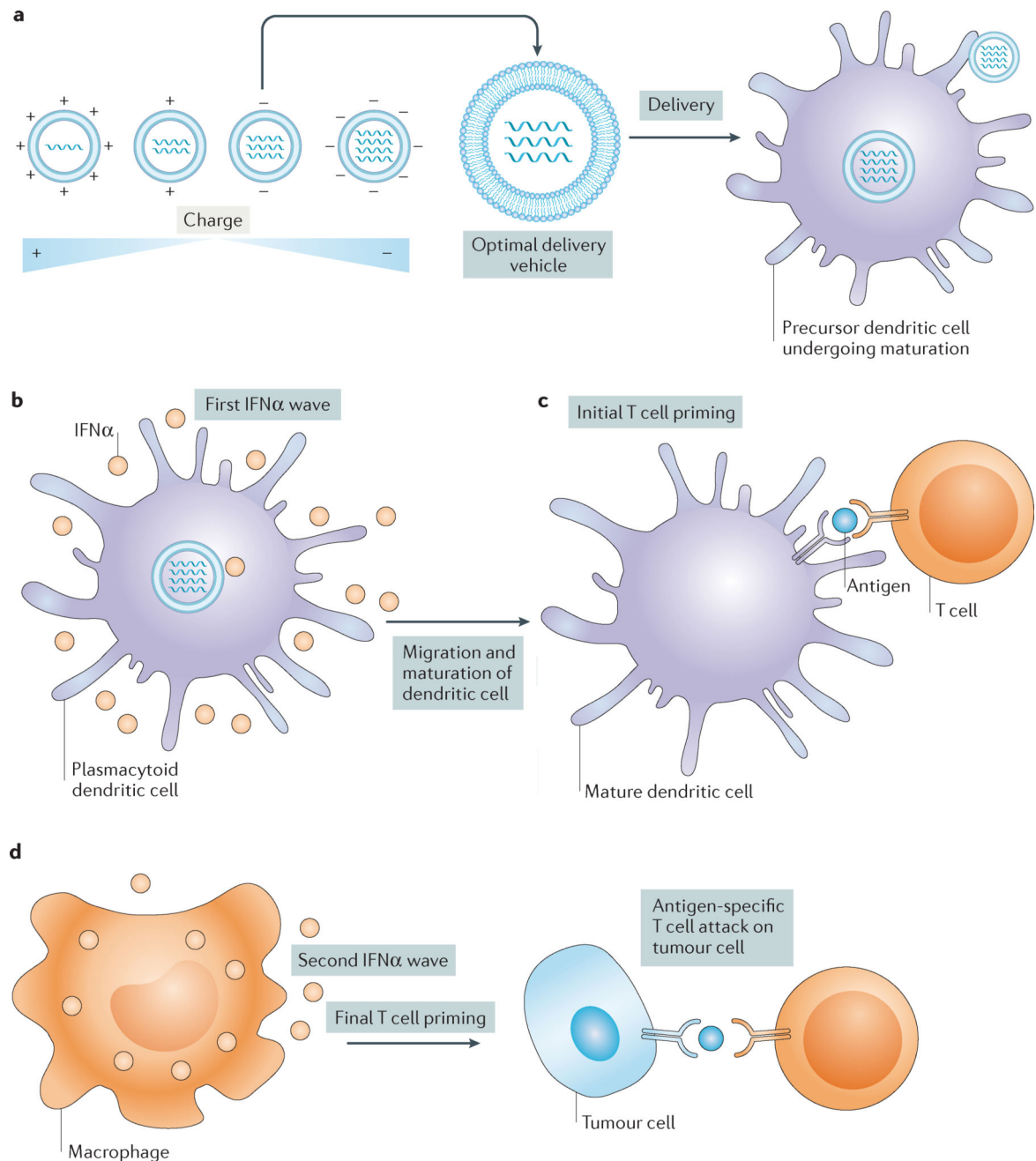


**Figure 4. Drug delivery vehicles to enhance cancer immunotherapy**

**a** | A nanoparticle library is engineered to have varying surface charge in the absence of targeting ligands. Nanoparticle charge is altered by tailoring the ratio of the lipid delivery material to the amount of encapsulated RNA. These materials are then screened in mice for efficient delivery and transfection of dendritic cells in the spleen and other lymphoid organs. The top candidate with a slightly negative charge is delivered into mice via a nanoparticle RNA vaccine to target precursor dendritic cells, which causes them to develop into mature antigen-presenting dendritic cells that migrate to the T cells in lymph nodes. **b** | Uptake by plasmacytoid dendritic cells promotes secretion of an initial wave of interferon- $\alpha$  (IFN $\alpha$ )

production that helps to prime initial T cell activation in lymph nodes<sup>98</sup>. **c** | Mature dendritic cells express tumour antigens derived from RNA, adjuvant or antigen in delivery vehicles and present them to T cells in lymph nodes. **d** | Uptake of delivery vehicles by macrophages leads to a second wave of IFN $\alpha$  release, fully priming T cells against specific antigens. Primed T cells then migrate to tumour sites, attacking and killing tumour cells. Figure from REF. 210, Macmillan Publishers Limited.

Author Manuscript

Author Manuscript

Author Manuscript

Author Manuscript

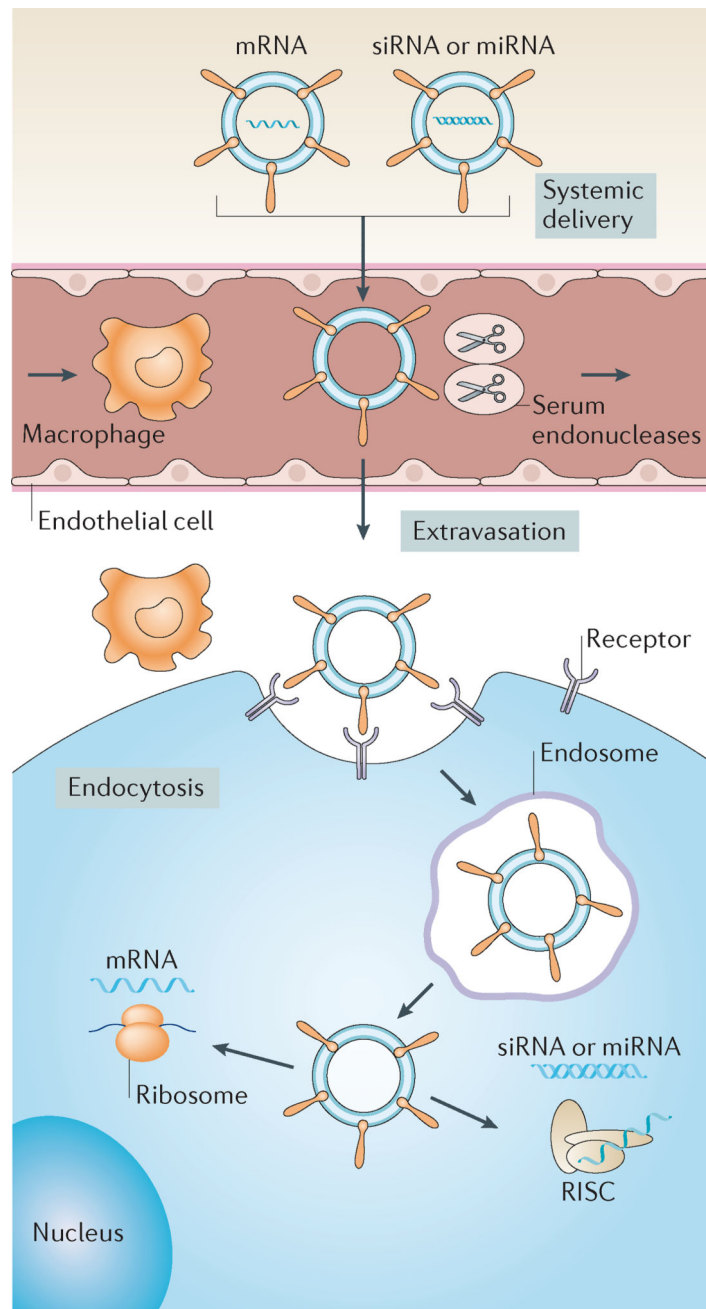


**Figure 5. Non-viral delivery vectors for RNA-based therapies**

Various non-viral vectors, such as nanoparticles, can be used to deliver mRNA, small interfering RNA (siRNA) or microRNA (miRNA) therapeutics to target cells *in vivo*. These vectors prevent degradation of nucleic acids by serum endonucleases and evade immune detection. For effective delivery, these vehicles need to avoid renal clearance from the circulation and prevent nonspecific interactions with cells and proteins. When delivered intravenously, these vectors need to (i) extravasate from the bloodstream to reach target tissues, owing to nanoparticle characteristics and/or targeting ligands, (ii) enter target cells via the plasma membrane and (iii) induce endosomal escape into the cytosol. siRNA and

miRNA must be loaded into the RNA-induced silencing complex (RISC) to initiate RNAi, whereas mRNA binds to translational machinery for subsequent protein expression. Figure from REF. 114, Macmillan Publishers Limited.

Author Manuscript

Author Manuscript

Author Manuscript

Author Manuscript

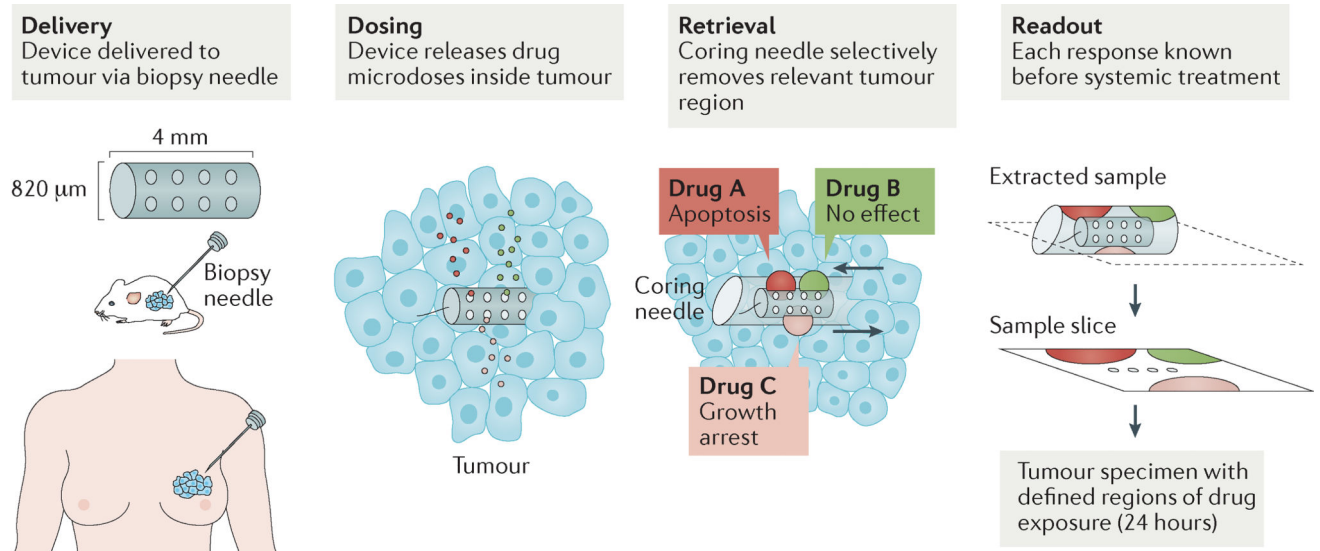


**Figure 6. Implantable drug delivery devices for simultaneous screening of many drugs in tumours**

Implantable drug delivery devices were recently developed to enable *in vivo* drug sensitivity testing and biomarker analysis in patient tumours. One such device that can be implanted directly into tumours via biopsy needle is shown. It can be used to administer and subsequently evaluate the effects of up to 16 different drugs simultaneously via drug-releasing microwells. Three drugs released from microwells are depicted here for simplicity. The drugs diffuse from the microwells into confined regions of the tumour. The tumour tissue is then biopsied using a second coring needle that retrieves the device itself and a small column of tissue adjacent to the device. This tissue contains regions exposed to the drugs and is used to evaluate drug effects, such as apoptosis or growth arrest<sup>124</sup>. Another delivery device, the CIVO platform (not shown in this figure), microinjects up to six different drugs into tumours as they are being withdrawn, leaving a 6 mm track of both the drug and inert tracking dye. Tumour cell death in response to drugs is assessed 24–72 hours after injection, via tumour resection. Evaluation of pharmacological and pharmacodynamic markers in these studies, such as cleaved caspase 3 as a marker of tumour cell apoptosis, demonstrated that device outputs were similar to the effects of systemic *in vivo* therapy<sup>125</sup>. These devices offer a possible alternative to the traditional way of using cancer drugs that has become accepted practice for clinical trials and animal research. Both devices potentially offer a personalized system for assessing drug sensitivity *in vivo* and tailoring therapy accordingly. Additionally, both devices provide ease of testing several drug combinations directly within tumours, along with probing inter-tumour and intra-tumour heterogeneity in their response to drugs. Figure from REF. 124: Jonas, O. *et al.* An implantable microdevice to perform high-throughput *in vivo* drug sensitivity testing in tumors. *Science Translational Medicine* **7**, 284ra57 (2015). Reprinted with permission from AAAS.

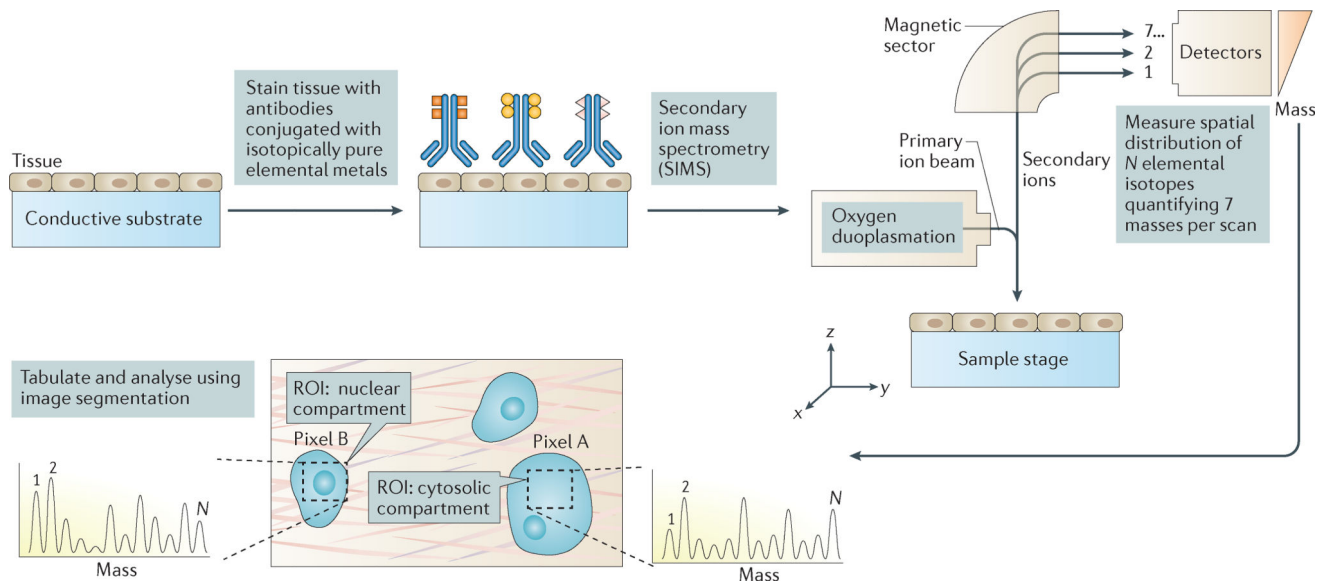
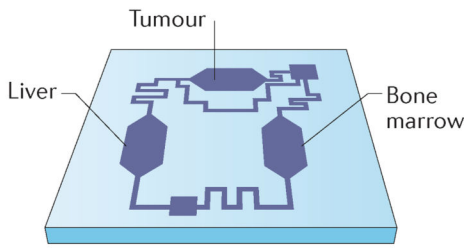


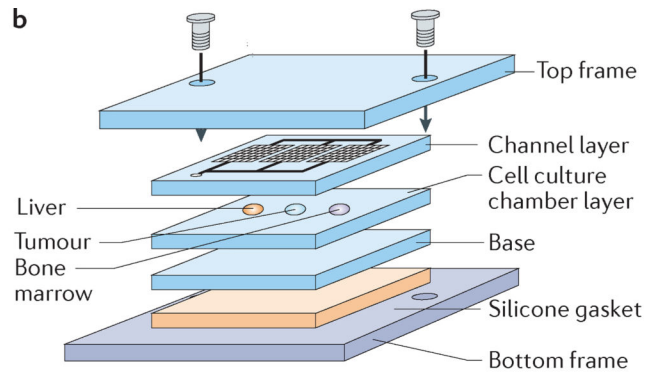
**Figure 7. Multiplexed ion beam imaging for detecting as many as 100 targets simultaneously in tumour tissue samples**

Cell and tissue samples are immobilized on a conductive substrate and subsequently stained with antibodies conjugated to unique, isotopically pure elemental metal reporters. Samples are then dried and loaded under vacuum for multiplexed ion beam imaging (MIBI) analysis, in which the surface is rasterized with an oxygen primary ion beam that sputters the antibody-specific metal reporters native to the sample surface as secondary ions. Metal-conjugated antibodies are quantified via replicate scans of the same field of view, and regions of interest (ROIs) demarcating nuclear and cytosolic compartments of cells within the sample are integrated, tabulated and categorized. From these expression data, composite images composed of pseudocoloured categorical features, and quantitative three-colour overlays are then constructed. MIBI is capable of detecting up to 100 unique isotope-labelled antibodies and has been used to analyse paraffin-embedded human breast cancer tissue samples stained simultaneously with ten isotope-labelled antibodies to detect features such as nuclear and cytosolic compartments of cells, providing new insights into disease pathogenesis for basic research and clinical diagnostics.  $N$  = number of unique elemental reporters. Figure from REF. 31, Macmillan Publishers Limited.

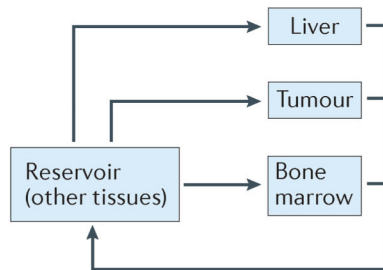
**a Micro cell culture analogue**



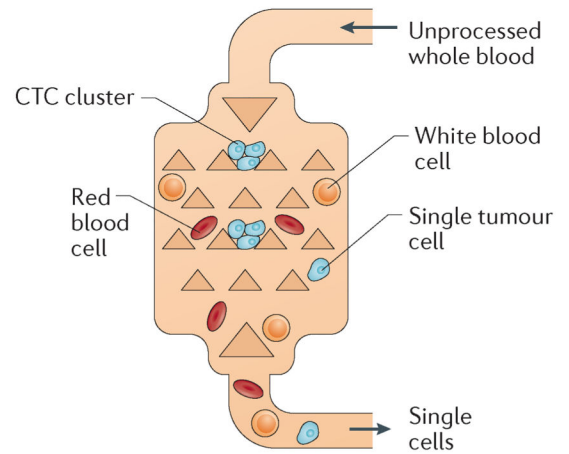
**b**



**c**



**d**



**e**

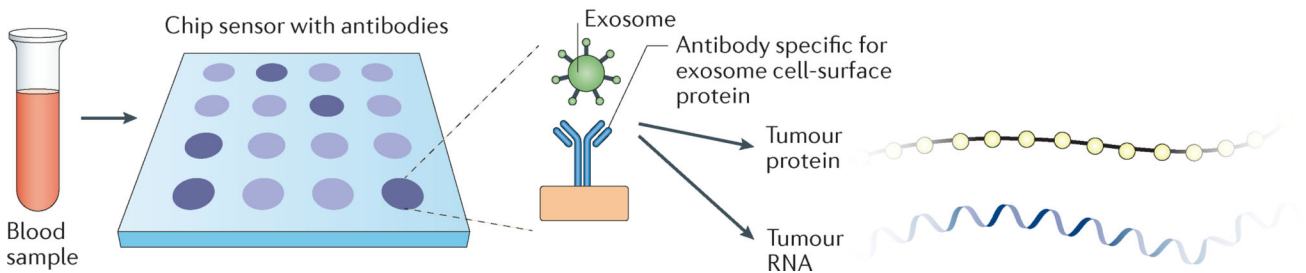


**Figure 8. Microfluidics and microfabricated devices for ‘organs-on-chip’ tumour models and cancer diagnostics**

**a** | A microfluidic device containing interconnected, 3D cell culture microchambers that mimic tissues (tumour, bone marrow, liver) to develop a multi-organ model that simulates absorption, metabolism and activity of chemotherapeutic agents. **b** | Schematic of the microfabrication of the three-chamber organs-on-chip that is linked via microfluidics. **c** | Flow diagram of the connections between the tumour, liver and bone marrow compartments of the microfluidic organs-on-chip model. Drugs are added into the culture medium, which is recirculated in a controlled manner through three inline chambers and an external reservoir, to mimic physiological blood flow rates and blood residence times in each organ. Mathematical models are also utilized for fitting to experimental toxicity measurements, and parameter optimization is used to mimic liver, tumour and bone marrow cytotoxicity *in*

*vivo*<sup>189</sup>. **d** | The Cluster-Chip device that captures circulating tumour cell (CTC) clusters from flowing unprocessed whole blood via microfabricated triangular micropillars, while single blood and tumour cells pass through the device<sup>200</sup>. **e** | Exosomes can be efficiently captured from blood using a nano-plasmonic exosome sensor, an array of periodic nanoholes patterned in gold film. Exosomes are captured on the sensors via affinity ligands specific for protein markers characteristic of exosomes, such as CD63. Exosome binding to the array changes the local refractive index of the sensor to an extent proportional to the level of the target protein, and can be used to detect the concentration of exosomes as well the abundance of proteins on or within exosomes<sup>204</sup>. As a result of this chip sensor technique, rare tumour proteins and RNA can then be extracted from exosomes for further analysis. Part a is from REF. 185, Macmillan Publishers Limited. Parts b and c are from REF. 15, Macmillan Publishers Limited. Part e is from REF. 211, Macmillan Publishers Limited.